Clim. Past, 7, 361–380, 2011
www.clim-past.net/7/361/2011/
doi:10.5194/cp-7-361-2011

Climate of the Past

Interglacial and glacial variability from the last 800 ka in marine, ice and terrestrial archives

N. Lang[1,*] **and E. W. Wolff**[1]

[1]British Antarctic Survey, High Cross, Madingley Road, Cambridge CB3 0ET, UK
[*]now at: National Isotope Centre, 30 Gracefield Rd, Gracefield, Wellington 5010, New Zealand

Received: 24 September 2010 – Published in Clim. Past Discuss.: 15 October 2010
Revised: 24 January 2011 – Accepted: 22 February 2011 – Published: 21 April 2011

Abstract. We have compiled 37 ice, marine and terrestrial palaeoclimate records covering the last 800 000 years in order to assess the pattern of glacial and interglacial strength, and termination amplitude. Records were selected based on their length, completeness and resolution, and their age models were updated, where required, by alignment to the LR04 benthic δ^{18}O stack. The resulting compilation allows comparison of individual glacial to interglacial transitions with confidence, but the level of synchronisation is inadequate for discussion of temporal phasing. The comparison of interglacials and glacials concentrates on the peaks immediately before and after terminations; particularly strong and weak glacials and interglacials have been identified. This confirms that strong interglacials are confined to the last 450 ka, and that this is a globally robust pattern; however weak interglacials (i.e. marine isotope stage 7) can still occur in this later period. Strong glacial periods are also concentrated in the recent half of the records, although marine isotope stage 16 is strong in many δ^{18}O records. Strong interglacials, particularly in the marine isotopic records, tend to follow strong glacials, suggesting that we should not expect interglacial strength to be strongly influenced by the instantaneous astronomical forcing. Many interglacials have a complex structure, with multiple peaks and troughs whose origin needs to be understood. However this compilation emphasises the under-representation of terrestrial environments and highlights the need for long palaeoclimate records from these areas. The main result of this work is the compiled datasets and maps of interglacial strength which provide a target for modelling studies and for conceptual understanding.

Correspondence to: N. Lang
(n.lang@gns.cri.nz)

1 Introduction

The climate of the recent third of the Quaternary is most clearly characterised by the alternation between cold glacial periods and warm interglacials; the dominant period of these climate cycles is 100 ka (e.g. Imbrie et al., 1993). In the four most recent climate cycles, the glacial periods are much longer than the interglacials. This climate signal is observed in marine sediments (Lisiecki and Raymo, 2005), in land records (Tzedakis et al., 2006) and in ice cores (Jouzel et al., 2007). The terms "glacial" and "interglacial" emphasise the changes in ice volume and sea level associated with the appearance and disappearance of large northern hemisphere ice sheets; however the general pattern is seen in numerous proxies related, for example, to temperature and the hydrological cycle, ocean conditions, and patterns of vegetation. The EPICA Dome C (EDC) ice core record shows that atmospheric composition, and in particular the concentrations of the greenhouse gases CO_2 and CH_4, has a similar pattern; these records were recently extended to 800 ka (Loulergue et al., 2008; Lüthi et al., 2008).

Understanding the causes of glacial-interglacial cycles requires not just replication of a "typical" glacial cycle, but an understanding of how slightly different external forcing and internal feedback mechanisms can lead to a wide range of responses. In recent years particular attention has been paid to the range of behaviours seen in interglacials (Tzedakis et al., 2009). The emergence of a longer ice core record has prompted a re-evaluation, reinforcing the view that each glacial-interglacial cycle has an individual pattern, which in the Antarctic ice cores is most clearly seen in interglacial variability (Jouzel et al., 2007). A first description (EPICA, 2004) was that interglacials before 450 ka ago were weak (cool) and long, while the more recent ones were strong and short. The implication is that a step change occurred around 430 ka ago (mid-Brunhes). However, with the new EDC3 age

Published by Copernicus Publications on behalf of the European Geosciences Union.

scale, the characterisation of length changes is less obvious, while closer examination reveals that there are differences between every interglacial in the Antarctic ice core record – not only in amplitude (Masson-Delmotte et al., 2010) but also in length or in profile (i.e. does it start warm and then cool, or vice versa). However we cannot understand the possible causes of these different patterns based on only regional records such as Antarctic temperature. The basis for such understanding and eventually for modelling the records as a response to the external forcing (Yin and Berger, 2010) has to be a characterisation of the global spatial signature for each interglacial and glacial, as well as the known forcing history that could have influenced it.

A further motivation for conducting a compilation now is that, for the first time, it is becoming possible to carry out transient model simulations of multiple glacial-interglacial cycles using Earth system models of intermediate complexity (EMICs) (Ganopolski and Calov, 2008; Holden et al., 2010). In addition serious attempts are now being made to use general circulation models of the ocean and atmosphere to simulate the climate of past interglacials with a strong emphasis on the last one (http://pmip3.lsce.ipsl.fr/). These modelling efforts require robust and clear targets, in particular emphasising the geographical pattern of climate in different periods. Although we will look in this paper at records covering the whole of the last 800 ka a major emphasis will be on interglacials because these warmer periods in Earth history are most relevant to the expected climate of the next century and beyond. In particular they provide a series of climates in which the hard-to-construct ice sheet forcing is relatively similar to that of the present and the other external forcings (astronomical and greenhouse gases) are rather well-known.They also appear to offer examples of climates warmer, at least in some critical regions, than that of the present, in which the response of the cryosphere, ocean circulation, and other components of the Earth system that are considered vulnerable to warmer climates can be assessed. However none of these gains can be realised unless we can compile representative sets of data across the globe and synchronise them to the level required for broad-scale model-data comparison.

Our approach in this paper will therefore be to identify and synthesise a set of as many regionally-representative records, on land, in the ocean, and in ice, as possible, where previous compilations (e.g. Masson-Delmotte et al., 2010) have focussed on either ice or marine records. The existence of the EDC ice core record motivates us to use a time period of 800 ka, encompassing the sequence of climate variability with a dominant cycle of 100 ka that has occurred since the Mid-Pleistocene Revolution (Mudelsee and Schulz, 1997) but not the cycles of 40 ka length that preceded it. The criteria for choosing the records are that they cover most of the last 800 ka, are continuous, and have a time resolution that allows the strength of interglacial peaks to be clearly characterised. Where there are several records from a region or representing a parameter of interest we have chosen the "best" one based on these criteria unless there is a reason to stack them. The quality of age controls does not allow a close synchronisation of records; however we have attempted to align the different records to ensure that common stages are being considered.

While we discuss the meaning of each proxy, we have derived the relative strengths of interglacials and glacials in each record based on the proxy values: in other words if the interglacial is characterised by a high (or low) value of a particular parameter compared to the glacial, then the interglacial with the highest (or lowest) value of that parameter is characterised as the strongest, without making judgments about what aspect of climate is represented. In this way we are able to make a ranking of interglacial (and glacial) strength for each site and proxy considered, and produce maps showing the pattern of relative strength for each interglacial (glacial). Such maps should provide an initial crude target for data-model comparisons. We are then able to make a first discussion of the profile of variables within interglacials as a precursor to more detailed studies in future.

2 Records used in the compilation

Large numbers of datasets cover multiple glacial-interglacial cycles, however relatively few are continuous and well-resolved. To merit inclusion here records must cover the entire 800 ka period we have chosen. Future studies of individual interglacials or of only the more recent climate cycles will be able to draw on a much wider sample of records, particularly in marine and terrestrial regions, but in order to characterise the relative strengths of interglacials and glacials without bias we have sacrificed quantity and areal coverage by requiring that each record must cover the entire period. The records must be of high enough resolution that trends within interglacials can be discerned and that some approximation to a maximum can be estimated without undue smoothing. In most cases we imposed a resolution limit of 2–3 ka; however, in order to include a reasonable range of sea surface temperature (SST) records, we relaxed the threshold to just over 4 ka in this case. It should be borne in mind that the low resolution at some periods makes our rankings (later in the paper) very uncertain for a few of the SST records. Finally records must be continuous, without any significant hiatuses or data gaps during the stages we are focussing on.

Two age scales have been particularly widely used and understood. In this compilation, the ice core age scale, EDC3 (Parrenin et al., 2007) has been used for all the ice core records. Marine data have been aligned to the LR04 age scale (Lisiecki and Raymo, 2005) as described (and with the caveats) in Sect. 2.4. LR04 and EDC3 appear to be rather well-aligned with each other (Parrenin et al., 2007), although there are certainly phase lags that have not been recognised. The result of this is that the data cannot be considered synchronised, probably within several thousand years.

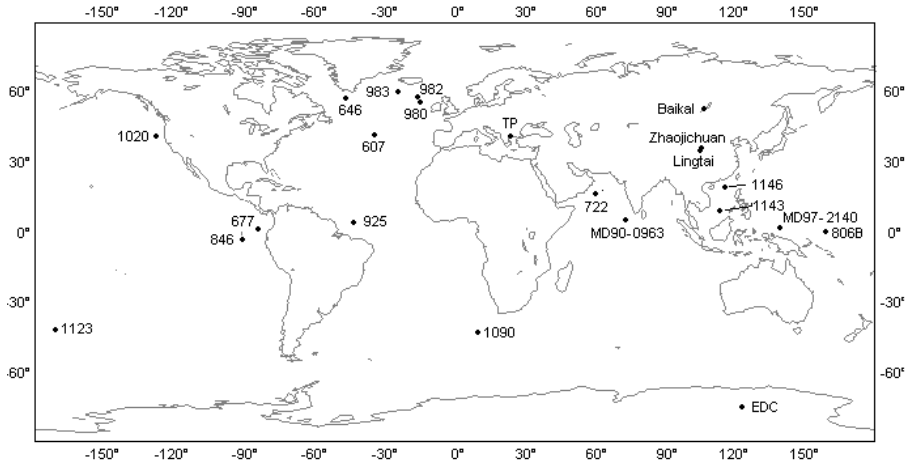

Fig. 1. Location of palaeoclimate records included in this synthesis.

Terrestrial records are presented on their own age scales. Nonetheless we are reasonably confident that the same marine isotope sub-stages are recognised in each record and can therefore be compared.

In addition to the observational data compiled here we have used calculations of insolation, obliquity and precession index (Laskar et al., 2004) using the Analyseries software (Paillard et al., 1996). The locations of each record used in our compilation are shown in Fig. 1 and the datasets are summarised in Table 1. All the records, after treatment as described below, are shown in Fig. 2.

2.1 Ice core records

The longest (in duration) Antarctic ice core record comes from the EPICA Dome C (EDC) ice core, covering the last 800 000 years (Jouzel et al., 2007; Parrenin et al., 2007). Other records covering several glacial-interglacial cycles are available from Vostok, reaching back 420 ka (Petit et al., 1999), and Dome Fuji, published so far to 340 ka (Watanabe et al., 2003; Kawamura et al., 2007), but with ice extending back to 740 ka ago under analysis. In their overlapping parts the three records show very similar characteristics despite some differences in amplitude, and we therefore treat the EDC records as being representative for East Antarctica. No records from Greenland or West Antarctica extend beyond a single glacial cycle.

The ice records presented here are on the EDC3 chronology (Parrenin et al., 2007), with ages in ka BP (thousands of years before 1950). The chronology was derived from a snow accumulation and mechanical ice flow model tuned to a set of independent age markers along the core, with quoted uncertainties of less than 1 ka at 18 ka, 1.5 ka at 40 ka, 3 ka at 100 ka and 6 ka between 130–800 ka.

The deuterium/hydrogen ratio in water molecules in ice is generally considered as a proxy for local temperature although the quantitative translation can be complex (Jouzel et al., 1997; Sime et al., 2009). The ratio is expressed using delta notation (δD) as permil deviations from a standard, with less negative values in interglacials. The EDC deuterium record (Jouzel et al., 2007) has been published at a depth resolution of 0.55 m; the age resolution expands from a decade near the surface to about 1 ka at 800 ka ago (averaging 0.14 ka).

CO_2 is a globally well-mixed gas due to its long lifetime, and therefore measurements made in Antarctica are globally representative and provide data for a very important climate forcing. Its concentration is driven over these timescales by changes both in the terrestrial biosphere, and in the ocean (physical and biological), with the Southern Ocean often considered to play a major role. Measurements from the gas phase of ice cores directly record the mixing ratios of CO_2 in air at the time of bubble close-off. The data here are actually a combination of measurements from the EDC and Vostok cores. CO_2 (Lüthi et al., 2008) was sampled irregularly with a resolution generally less than 1 ka (average 0.7 ka), and a quoted analytical uncertainty of 1.5 ppmv.

CH_4 has a shorter lifetime than CO_2 and therefore shows an inter-hemispheric gradient. Nonetheless changes in CH_4 in Antarctica represent global changes and to first order the EDC record can be considered globally representative of this greenhouse gas, which responds to changes in terrestrial sources and atmospheric sinks. The sources and sinks are mainly found in the northern high latitudes and the tropics so that CH_4 should be responding to some aspects of climate in these regions (it is beyond the scope of this paper to define this further). The EDC CH_4 record (Loulergue et al., 2008) is also sampled irregularly but generally with a resolution better than 1 ka (average 0.38 ka) over the last 800 ka, with a quoted analytical uncertainty of 10 ppbv. Both gases show high concentrations during interglacials; remembering our method of characterising interglacial and glacial strength, discussed in

Table 1. Palaeoclimate records included in this synthesis.

Site/record	Parameter	Location	Resolution*	References
EDC	CO_2 concentration	East Antarctica	0.8 ± 0.7	Loulergue et al. (2008)
	CH_4 concentration		0.4 ± 0.3	Lüthi et al. (2008)
	δD		1.0	Jouzel et al. (2007)
LR04	δ^{18}O (b)	Global stack	ka average	Lisiecki and Raymo (2005)
DSDP 607	Mg/Ca BWT	North Atlantic	4.1 ± 2.8	Sosdian and Rosenthal (2009)
	SST (foram assemblage)		2.2 ± 1.7	Ruddiman et al. (1989)
ODP 646	δ^{18}O (p)	North Atlantic	2.6 ± 1.0	de Vernal and Hillaire-Marcel (2008)**
ODP 677	δ^{18}O (b/p)	East Equatorial Pacific	$2.5 \pm 1.3/2.4 \pm 1.2$	Shackleton and Hall (1989)
ODP 722	$U^{k'}_{37}$SST	Indian Ocean	1.7 ± 0.9	Herbert et al. (2010)
ODP 806B	δ^{18}O (p)	West Equatorial Pacific	2.3 ± 2.2	Medina Elizalde and Lea (2005)
	Mg/Ca SST		2.3 ± 2.2	
ODP 846	δ^{18}O (b)	East Equatorial Pacific	2.5 ± 1.6	Mix et al. (1995)
	$U^{k'}_{37}$ SST		2.3 ± 1.3	Liu and Herbert (2004)
ODP 925	δ^{18}O (b)	West EquatorialAtlantic	2.4 ± 1.6	Bickert et al. (1997)
ODP 980	δ^{18}O (b)	North Atlantic	0.7 ± 0.7	Raymo et al. (2004)
ODP 982	δ^{18}O (b / p)	North Atlantic	$2.3 \pm 1.5/2.0 \pm 1.0$	Venz and Hodell (1999)
	$U^{k'}_{37}$SST		4.6 ± 3.0	Lawrence et al. (2009)
ODP 983	δ^{18}O (b)	North Atlantic	0.9 ± 1.5	Raymo et al. (2004)
ODP 1020	$U^{k'}_{37}$SST	North East Pacific	2.2 ± 0.8	Herbert et al. (2001)
ODP 1090	δ^{18}O (b/p)	Southern Ocean	$1.7 \pm 1.7/1.2 \pm 0.6$	Hodell et al. (2003)
	U^{k}_{37} index SST		2.4 ± 1.7	Martinez-Garcia et al. (2009)
ODP 1123	δ^{18}O (b)	Southern Ocean	2.4 ± 0.8	Hall et al. (2001)
	SST (foram assemblage)		2.4 ± 0.8	Crundwell et al. (2008)
ODP 1143	δ^{18}O (b)	South China Sea	2.4 ± 1.9	Tian et al. (2002)
ODP 1146	δ^{18}O (b/p)	South China Sea	$2.0 \pm 1.4/1.7 \pm 1.1$	Clemens and Prell (2004)
	$U^{k'}_{37}$SST		1.7 ± 1.1	Herbert et al. (2010)
MD90-0963	δ^{18}O (p)	Indian Ocean	2.1 ± 1.3	Bassinot et al. (1994)
MD97-2140	Mg/Ca SST	West Equatorial Pacific	4.0 ± 2.8	de Garidel-Thoron et al. (2005)
Zhaojichuan/	Mass accumulation rate	Chinese Loess Plateau	1	Sun and An (2005)
Lingtai	Magnetic susceptibility		1	
LakeBaikal	Biogenic silica	Southern Siberia	0.5 ± 0.2	Prokopenko et al. (2006)
Tenaghi Philippon	Arboreal pollen	Greece	1.3 ± 0.7	Tzedakis et al. (2006)

*Resolution (in ka) averaged over the last 800 ka, b = benthic, p = planktonic, BWT = bottom water temperature, SST = sea surface temperature. The LR04 stack "ka average" refers to the 1 ka intervals over which points from the individual datasets were averaged.
**Based on data in Aksu et al. (1989).

the introduction, this means that interglacials (glacials) with higher (lower) concentrations are described as "stronger" for this proxy in the tables and figures that follow.

Other measures such as sea salt and terrestrial dust components (Wolff et al., 2010) have been analysed in the EDC core. Sea salt flux is often interpreted as representing sea ice extent; in interglacials it more or less shadows deuterium although it seems to saturate at high (glacial) sea ice extents (Rothlisberger et al., 2010). Terrestrial dust components seem to exhibit a threshold with consistent low fluxes in interglacials. We do not include either component in this compilation but their relative strengths have been discussed elsewhere (Masson-Delmotte et al., 2010).

2.2 Terrestrial records

Only a very small number of continental records met our criteria for length, resolution and completeness. We were unable to locate any suitable records from Australasia, Africa or North America. Long records of pollen from Colombia in South America have been published (Hooghiemstra et al., 1993). We understand that the age scale is currently being re-assessed (Hooghiemstra, personal communication, 2008) and decline to include the data while this is in progress; it is also difficult to interpret data from any simple metric at this site due to background trends imposed by the arrival in the record of new (to the region) species. This leaves us with a

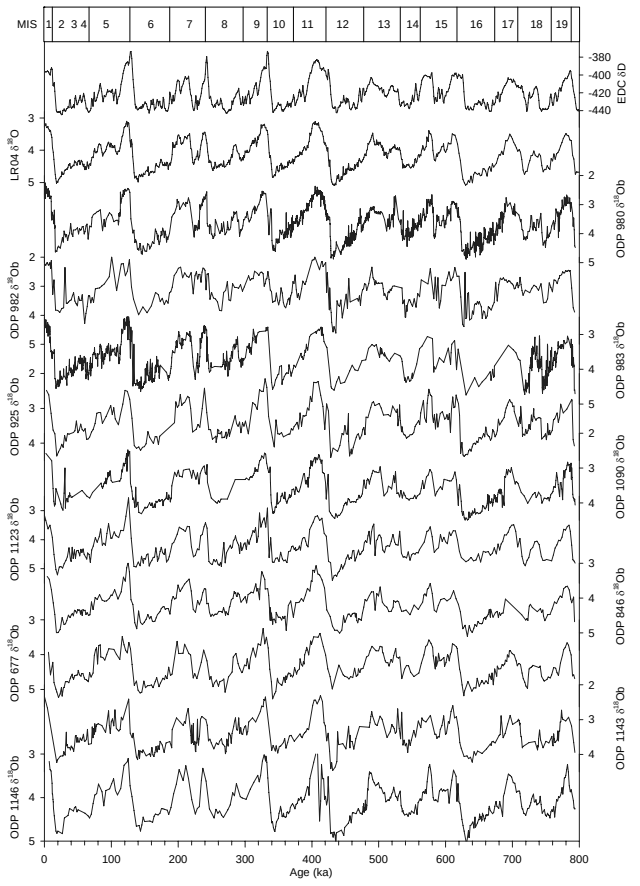

Fig. 2a. Benthic δ^{18}O records aligned to the LR04 benthic stack, with corresponding marine isotope stages (MIS) from LR04; EDC δD on EDC3 timescale.

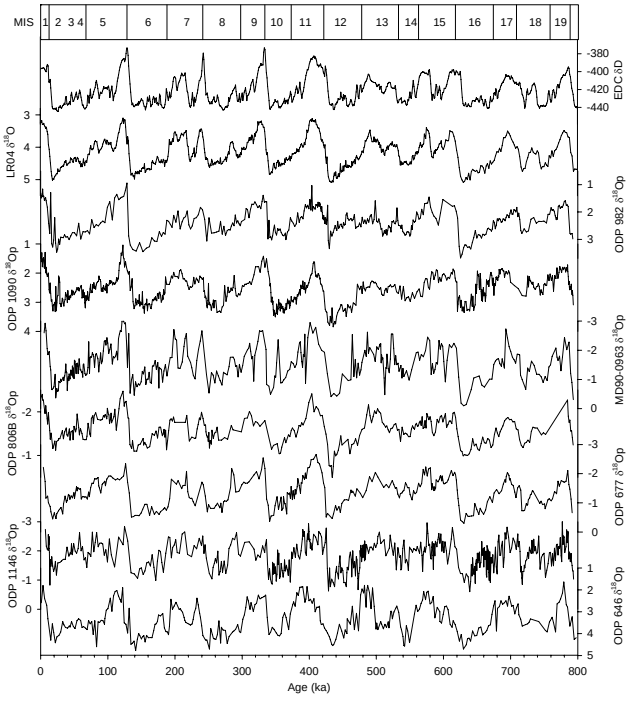

Fig. 2b. Planktonic δ^{18}O records aligned to the LR04 benthic stack, with corresponding marine isotope stages (MIS) from LR04; EDC δD on EDC3 timescale.

single long pollen record from Europe, and Asian loess and lacustrine data. Increasingly, higher resolution pollen counts are being published from marine cores (e.g. Sun et al., 2003) which offer the opportunity to look at regional climate from pollen, due to the larger source area of marine sites than terrestrial pollen records. However those we are aware of have a low resolution or are discontinuous and therefore have not been included in this compilation. A recent record contains a pollen dataset for a site (ODP 646) just south of Greenland. This dataset is interpreted (de Vernal and Hillaire-Marcel, 2008) as a record of vegetation development related to ice sheet volume in southern Greenland. Because this rather specialist interpretation is of a different nature to the more general climate proxies we are considering, we do not present this record among our terrestrial proxies here, but we do refer to the record in the text.

Biogenic silica content (BioSi %) of Lake Baikal sediments records changes in the lake's diatom productivity (Prokopenko et al., 2006) with high values during interglacials. The record spans the last 1.8 Ma, with an average resolution of 0.5 ka over the last 800 ka. The age model was constructed by orbitally tuning the record based on the correlation of peak BioSi %, which is likely controlled by the lake heat balance and thermal stratification (Prokopenko et al., 2001; Prokopenko et al., 2006), with September perihelia during interglacials.

The arboreal pollen (AP) % curve from Tenaghi Philippon, NE Greece extends back ∼1.35 Ma (Tzedakis et al., 2006) at an average resolution of 1.3 ka for the last 800 ka. The astronomical timescale was developed by the identification of initial anchor points from a composite benthic δ^{18}O curve ("S06") and orbital tuning of the AP% record using two features (Magri and Tzedakis, 2000): tree population crashes (i.e. AP% minima) during cold and dry episodes at March perihelion, and expansion of Mediterranean vegetation (i.e. peaks in *Pistacia* during early temperate phases) during maximum summer temperature/evaporation regimes at June perihelion. High AP% is seen during interglacials.

A number of loess mass accumulation records (MAR, g cm^{-2} ka^{-1}) are available from the Chinese Loess Plateau, potentially extending back 7 Ma (Sun and An, 2002; Kohfeld and Harrison, 2003). Variation in the accumulation of loess is linked to variability in the East Asian monsoon and continental aridity in central Asia, with increased accumulation during glacials and paleosol development during interglacials. Sites in Zhaojichuan and Lingtai provide a continuous record of the last 800 ka, with a resolution of 1.2 ka (Sun and An, 2005), and we include stacked MAR and

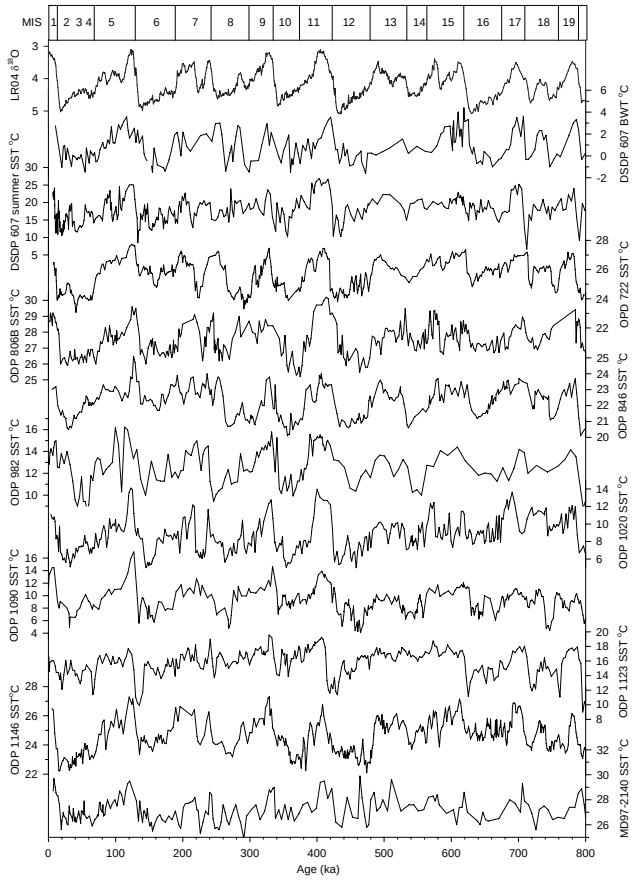

Fig. 2c. Sea surface temperature (SST) records (on individual timescales) with corresponding marine isotope stages (MIS) from LR04.

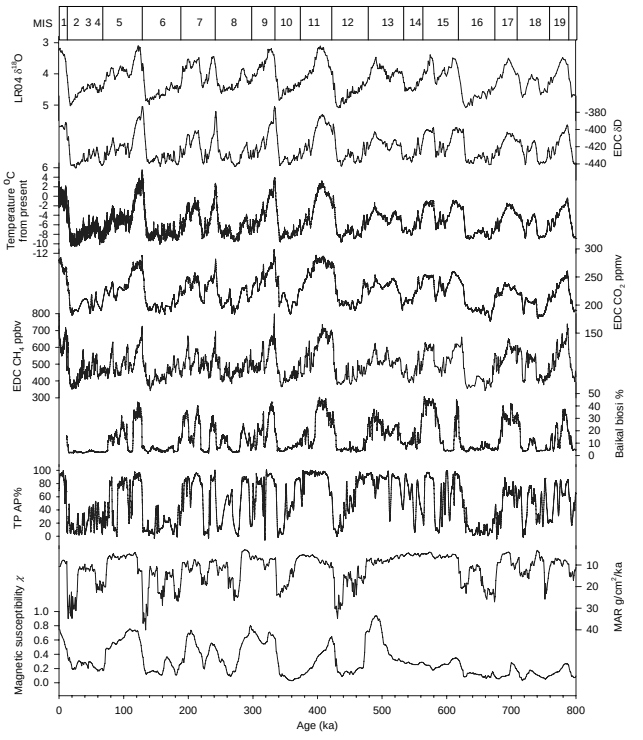

Fig. 2d. EPICA Dome C records on EDC3 timescale, and terrestrial records (on individual timescales); LR04 benthic stack and corresponding marine isotope stages (MIS) from LR04.

stacked magnetic susceptibility (MS) for these two sites. The original timescale was constructed by orbitally tuning the mean quartz grain size record from the sites to obliquity and precession targets (Sun et al., 2006). While loess accumulation is higher and more variable during glacials, MAR is not a sensitive recorder of interglacial variability. High magnetic susceptibility is associated with paleosol development, due to the production of fine-grained magnetic minerals in paleosols during pedogenesis in warmer/wetter periods; however other factors affect magnetic susceptibility and so it is wise to use these data in conjunction with other datasets from the same sequences (Bloemendal et al., 2008).

2.3 Marine records

Because it is so widely measured most of the marine datasets we have used are of δ^{18}O. Ten records of benthic foraminiferal δ^{18}O and seven of planktonic foraminiferal δ^{18}O are included from marine sediment cores. Foraminiferal δ^{18}O varies as a function of the temperature and δ^{18}O of seawater, and δ^{18}O of seawater as a function of its local salinity and global ice volume; benthic δ^{18}O is generally considered to be controlled mainly by global ice volume and deepwater temperature, while planktonic δ^{18}O has a more significant local overlay from local salinity and SST.

The LR04 stack (Lisiecki and Raymo, 2005), which is composed of 57 globally distributed records of benthic foraminiferal δ^{18}O, is included for comparison. We note that only a small minority of the records used in LR04 meet our criteria for inclusion as individual records in this compilation primarily due to low resolution, and that the number of records in LR04 decreases strongly with increasing age. The 57 records in LR04 were aligned using an automated graphic correlation algorithm, Match (Lisiecki and Lisiecki, 2002), and the resulting stack (averaged over 1 ka intervals) placed on a timescale by tuning to a simple ice volume model (Imbrie and Imbrie, 1980), using values for 21 June insolation at 65° N (Berger and Loutre, 1991). The quoted confidence interval in the LR04 age model is estimated to be 4 ka between 1 Ma and present (Lisiecki and Raymo, 2005). Age differences of up to 6 ka between the EDC3 and LR04 models have been identified by comparing features that could be confidently identified in each record (i.e. midpoints of each termination) (Parrenin et al., 2007); this uncertainty is small enough that we can be confident that we have lined up the same marine isotope stages (MIS) in records synchronised to each of these age scales, even though the exact timing of

maxima and minima may be in doubt. As the age models of the 17 δ^{18}O records presented here vary in their methods of construction and in some cases are outdated, the records were converted to the LR04 timescale by alignment with the stack (next section).

Records of sea surface temperature (SST) can be derived in various ways. Ten SST records meet our criteria and are included. SST data from site MD97-2140 (de Garidel-Thoron et al., 2005) and ODP site 806B (Medina Elizalde and Lea, 2005) are derived from foraminiferal Mg/Ca palaeothermometry, based on the temperature-dependent substitution of Mg in calcite; while at ODP sites 722 and 1146 (Herbert et al., 2010), 846 (Liu and Herbert, 2004), 982 (Lawrence et al., 2009), and 1020 (Herbert et al., 2001) the unsaturation index ($U^{k'}_{37}$) of alkenones produced by coccolithophores provides a means of deriving mean annual SST. For ODP site 1090, an alternative measure derived from alkenones, the U^K37 palaeotemperature index, has been used as it is better correlated with mean annual SST at higher latitudes (Martinez-Garcia et al., 2009). SST at ODP site 1123 is derived from planktonic foraminiferal assemblage data using MAT and ANN approaches (Crundwell et al., 2008), and DSDP 607 SSTs for summer and winter (Sosdian and Rosenthal, 2009) are based on foram census counts from (Ruddiman et al., 1989). Bottom water temperatures (BWT) from DSDP site 607 (Sosdian and Rosenthal, 2009) are also calculated from foraminiferal Mg/Ca palaeothermometry.

Quoted confidence intervals for these methods vary but are typically $\leq \pm 0.5\,^{\circ}$C ($\pm 0.06\,^{\circ}$C for sites 722 and 1146; $\pm 0.15\,^{\circ}$C for 1020; $\pm 0.2\,^{\circ}$C for 982, 806B and 846; and $\pm 0.5\,^{\circ}$C for site 1090 and MD97-2140), with the exception of site 607 ($\pm 1.1\,^{\circ}$C for BWT and $\pm 2\,^{\circ}$C for SST).

There is an abundance of δ^{13}C (carbonate) data from marine cores, often of suitable resolution for inclusion. However the δ^{13}C climate signal is more complex and less well understood than δ^{18}O. For this reason, these records are not included in this synthesis. Recent compilations of the last 150 000 and 425 000 years perhaps point the way to a more comprehensive effort for a longer period (Lisiecki and Raymo, 2008; Oliver et al., 2010).

2.4 Alignment of δ^{18}O and SST records to the LR04 stack

For the purposes of this paper the δ^{18}O and SST records discussed in the previous section have been converted to a single timescale, LR04 (Lisiecki and Raymo, 2005), using an automated graphic alignment program, Match (Lisiecki and Lisiecki, 2002). Alignment of the records ensures that the same feature is being identified in each. This type of graphic correlation assumes that sites record the same benthic δ^{18}O signal with little phase difference, while in reality there is evidence that significant lags do exist: the timing of benthic δ^{18}O change at the last termination differed by 4000 years between two sites in the Atlantic and Pacific (Skinner and Shackleton, 2005), although a smaller lag (Pacific δ^{18}O lagging Atlantic by an average of 1.6 ka, increasing to 4 ka during some terminations) has also been reported for the last five terminations (Lisiecki and Raymo, 2009). In this paper it is the strength, and not the phasing, of the signal that is being considered, so the correlation procedure seems appropriate.

Benthic δ^{18}O records from ODP sites 677, 846, 925, 980, 982, 983, 1090, 1123, 1143, and 1146 were individually aligned to the LR04 δ^{18}O stack, using 0 ka (or the top of the core) and the MIS 19–20 transition as tie-points. The records were first normalised to maximize the accuracy of the Match algorithm. Match uses penalty functions to ensure that alignments result in sediment accumulation rates and changes in rates that are physically realistic. Using the depths and ages from the converted benthic records as age control points, the planktonic records from ODP sites 677, 982, 1090, and 1146 were then converted to the LR04 timescale using a linear interpolation macro (S. Crowhurst, personal communication, 2008). This preserves the relationship between benthic and planktonic records from the same core, while direct alignment of the planktonic records to LR04 using Match would force them into phase. Planktonic records from sites 806B, 646 and MD90-0963 were directly aligned to the LR04 benthic stack. Site 806B, 846 and 1123 SST records are also aligned with LR04 by comparison with the sites' δ^{18}O records, while MD97-2140 SST was aligned directly with LR04 δ^{18}O. The age model for site 1090 SST varies from that of the δ^{18}O record from the same core. SST was aligned with the EDC temperature record (on the EDC3 timescale) using Analyseries (Martinez-Garcia et al., 2009); as the differences between the LR04 and EDC3 timescales have been evaluated, this record is left on this timescale and not aligned to LR04 using Match. Age models for SST records from sites 607, 722, 982, 1020, and 1146 were constructed by alignment with LR04 by their original authors, and so have been used here on their published timescales.

Sedimentation rates were calculated for the converted records, and the converted records compared with the originals to ensure that each alignment is realistic (Table 2). The age difference between the LR04 and original timescales is most noticeable for sites 806B, 980, 982, 983, and 1143 where the original age models were constructed using the benthic record and age model of site 677 (or composites including site 677 e.g. S95), which is up to 20 ka younger than LR04 between 400–590 ka (Lisiecki and Raymo, 2005).

2.5 Indexing interglacial and glacial maxima

Each glacial-interglacial transition for Terminations I to IX was looked at in order to identify the glacial minimum, interglacial maximum and termination amplitude (the difference between maximum and minimum). We have taken the termination as traditionally defined, i.e. at the change from an even- to an odd-numbered marine isotopic stage. In one place this departs from a recent usage: for Termination VIII, we

Table 2. Sediment accumulation rates from LR04 and original age models, and maximum age differences (Δ age) between the two models.

Site	Δ age	Original sed. rate ($m\,ka^{-1}$)	LR04 sed. rate ($m\,ka^{-1}$)
ODP 677	29 ka	0.01–0.12	0.01–0.10
ODP 806B	20 ka	0.003–0.06	0.003–0.08
ODP 1090	17 ka	0.01–0.07	0.01–0.09
ODP 846	17 ka	0.02–0.07	0.01–0.08
ODP 925	16 ka	n/a	0.02–0.06
ODP 980	16 ka	0.03–0.43	0.03–0.42
ODP 982	16 ka	0.01–0.08	0.01–0.08
ODP 646	16 ka	0.01–0.23	0.01–0.22
ODP 983	11 ka	0.02–0.54	0.02–0.40
ODP 1123	10 ka	0.03–0.05	0.02–0.06
ODP 1143	10 ka	0.01–0.25	0.01–0.32
ODP 1146	8 ka	0.05–0.50	0.03–0.40

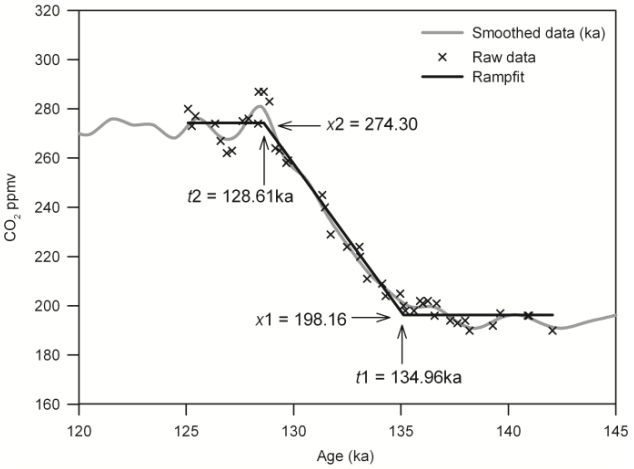

Fig. 3. Comparison of methods for determining peak glacial and interglacial values and termination amplitude, using EDC CO_2. The glacial ($x1$) and interglacial ($x2$) values (in ppmv), and the beginning ($t1$) and end ($t2$) of the termination, are shown as calculated by Rampfit.

have taken the transition from MIS 18 to MIS 17 starting at around 718 ka on the LR04 age scale. In a recent paper looking at the relative behaviour of Na, Ca and δD across terminations in ice cores, the transition starting at around 746 ka (between marine isotope events 18.4–18.3 in the nomenclature of Bassinot et al., 1994) was considered and was (in traditional terms, incorrectly) labelled as TVIII. The difficulty of clearly defining glacial and interglacial periods in some parts of the record is further discussed in relation to the MIS13-15 period later.

The minima and maxima identified were those nearest to the transition, and therefore do not necessarily correspond to the absolute maximum or minimum within a particular stage. These values were identified (a) in the raw data, i.e. single point maxima and minima were included; (b) in records averaged to 1 ka to ensure we were considering sustained values in the records with highest resolution, and (c) using the statistical RAMPFIT programme to determine the values of maxima and minima (Fig. 3). Rampfit (Mudelsee, 2000) fits a "ramp", which is a continuous function segmented in three parts: $x_{\mathrm{fit}}(t) = x1$ for $t \leq t1$, $x2$ for $t \geq t2$, and linearly connected between $t1$ and $t2$, to the data. The unknowns $x1$ (glacial value) and $x2$ (interglacial value) are estimated by weighted least-squares regression, $t1$ and $t2$ by a brute-force search. By fitting a best-fit ramp to each transition, "average" values can be calculated for the early-interglacial and late-glacial maxima. Selection of the fit interval for the ramp is subjective, and so the criterion for the selected interval was that the start and end points should be within a section of data with a small deviation from a constant level (i.e. the interglacial and glacial sections have a small standard deviation). Multiple runs were made with different intervals to test the sensitivity of $x1$ and $x2$ to interval length. The differences in the strength of interglacials (glacials) found using each of these three methods were not significant, and all results shown in this paper are from the raw data.

Maximum (raw) values for each interglacial in each record are presented in Table 3. For each record, each of the nine interglacials (or, in Tables 4 and 5, glacials, or termination amplitudes) is then colour-coded (in the table) according to strength, running from dark red to light red (dark blue to light blue for the strength of glacials, and dark purple to light purple for the amplitude of terminations), with the difference in shading between interglacials defined by where their values are on the continuum between strongest and weakest. The colour coding in the tables is provided to emphasise the trends in these large datasets. We again emphasise that we used the value of the proxy, defining that if a proxy becomes more positive (negative) in moving from glacial to interglacial, then the more positive (negative) the interglacial value is, the stronger the interglacial (the strongest interglacial is colour-coded as the darkest red, and the weakest as the lightest). The coding of strongest glacials and termination amplitudes was calculated using a similar logic. This makes no judgment about the interpretation of the proxy, but assesses the relative interglacial (glacial) strength of the proxy value itself.

3 Interglacial and glacial maximum strength

The variation in normalised peak interglacial values in the marine (and ice core) records is around 40% (60%) of that of the maximum glacial-interglacial change (Fig. 4), which implies that there is reasonable interglacial discrimination in most records. By contrast while different glacials show significant differences in the marine data, there is relatively

Table 3. Maximum (post-termination) values for each interglacial. The values are colour-coded according to strength, with deep red being the strongest, and pale red the weakest, interglacial signal for each palaeoclimate record.

Interglacial			MIS 1	MIS 5	MIS 7	MIS 9	MIS 11	MIS 13	MIS 15	MIS 17	MIS 19
MARINE	BENTHIC $\delta^{18}O$	ODP 677	*	3.65	3.87	3.25	3.39	3.82	3.69	3.89	3.66
		ODP 846	3.38	2.98	3.73	3.25	3.07	4.07	3.79	4.03	3.66
		ODP 925	2.48	2.46	2.42	2.15	2.23	2.90	2.62	2.75	2.74
		ODP 980	2.25	2.44	2.56	2.54	2.37	2.70	2.89	2.76	2.67
		ODP 982	2.11	2.09	2.56	2.49	1.99	2.99	2.35	2.69	2.46
		ODP 983	2.59	2.40	2.74	2.79	2.79	3.54	3.17	3.31	3.05
		ODP 1090	2.58	2.48	2.90	2.57	2.61	3.10	3.11	2.99	2.83
		ODP 1123	3.16	2.56	3.42	2.91	3.18	3.71	3.69	3.49	3.50
		ODP 1143	2.34	2.41	2.91	2.35	2.31	2.69	2.60	2.88	2.93
		ODP 1146	3.17	3.10	3.33	3.02	2.94	3.85	3.37	3.46	3.24
		LR04	3.18	3.10	3.44	3.19	3.11	3.83	3.49	3.50	3.48
	PLANKTONIC $\delta^{18}O$	ODP 646	1.80	1.90	2.38	2.24	1.85	2.74	2.06	2.29	1.64
		ODP 677	*	-2.00	-0.72	-2.41	-2.65	-0.83	-1.54	-0.48	-1.54
		ODP 806b	-2.40	-2.47	-1.99	-2.01	-2.41	-1.73	-1.99	-1.87	-2.27
		ODP 982	1.28	0.94	1.83	1.39	1.75	1.85	1.54	1.83	1.59
		ODP 1090	1.29	1.04	2.10	1.42	1.61	2.39	1.86	1.92	1.72
		ODP 1146	-2.74	-2.84	-2.51	-2.38	-2.78	-2.37	-2.80	-2.58	-2.72
		MD90-0963	-2.93	-3.13	-2.67	-2.68	-2.95	-2.56	-2.24	-1.87	-2.44
	SST (°C)	DSDP 607s	23.10	25.10	20.50	23.60	26.60	22.30	22.90	25.20	24.00
		DSDP 607w	16.20	17.40	13.80	16.40	19.50	15.20	16.10	18.20	16.80
		ODP 722	26.50	27.71	27.26	27.47	27.46	26.16	27.37	27.20	27.11
		ODP 806B	29.20	29.60	29.20	28.80	30.20	29.48	28.74	28.46	29.42
		ODP 846	23.20	25.10	23.80	23.80	24.00	23.20	23.50	23.70	23.70
		ODP 982	14.98	16.23	14.49	15.79	15.03	13.26	14.40	14.20	14.14
		ODP 1020	11.10	14.10	11.66	12.76	13.98	10.13	11.46	13.63	12.13
		ODP 1090	14.51	17.14	10.22	14.67	13.93	10.24	12.07	11.07	10.35
		ODP 1123	16.55	17.71	18.99	19.56	19.26	17.86	17.41	18.04	17.93
		ODP 1146	26.49	27.29	26.27	27.31	26.78	25.68	27.15	26.68	26.16
		MD97-2140	29.70	29.50	28.60	29.00	29.50	29.60	28.60	29.30	28.90
	BWT	DSDP 607	*	3.60	3.00	2.90	3.50	1.50	4.40	3.60	3.30
ICE		δD (‰)	-392	-374	-380	-373	-383	-412	-398	-403	-395
		CO_2 (ppmv)	285	287	280	299	289	248	260	240	260
		CH_4 (ppbv)	717	726	696	797	736	541	661	652	739
TERRESTRIAL	LOESS	MAR stacked	7.80	4.21	7.52	6.68	8.87	**	4.97	4.02	6.89
		MS stacked	0.75	0.73	0.56	0.71	0.65	0.94	0.33	0.28	0.27
		TP (%)	99.48	96.76	96.70	95.50	98.43	91.43	95.18	82.20	83.27
		Baikal (%)	*	43.1	32.3	43.0	46.0	26.2	43.8	42.1	34.5

*Top of core missing
** Stage not clearly resolved

Table 4. Maximum (pre-termination) values for each glacial. The values are colour-coded according to strength, with dark blue being the strongest, and pale blue the weakest, glacial signal for each palaeoclimate record.

Glacial			MIS 2	MIS 6	MIS 8	MIS 10	MIS 12	MIS 14	MIS 16	MIS 18	MIS 20
MARINE	BENTHIC $\delta^{18}O$	ODP 677	5.23	5.10	4.92	5.27	4.99	4.69	5.18	4.97	4.69
		ODP 846	4.99	4.88	4.53	4.75	5.01	4.48	5.10	4.64	4.68
		ODP 925	4.37	4.21	3.98	4.11	4.41	3.86	4.38	3.80	4.08
		ODP 980	4.63	4.71	4.17	4.61	4.87	4.44	4.88	4.22	4.48
		ODP 982	3.90	3.98	3.45	3.56	4.61	4.06	4.39	3.31	3.89
		ODP 983	4.55	4.46	4.08	4.57	4.60	4.37	4.74	4.72	4.70
		ODP 1090	4.09	4.31	4.01	4.30	4.45	3.92	4.49	4.01	4.06
		ODP 1123	5.21	4.94	4.86	4.78	5.40	4.71	4.76	4.90	4.81
		ODP 1143	4.23	4.15	3.84	3.88	4.46	3.94	4.22	3.81	3.94
		ODP 1146	4.82	4.77	4.47	4.78	5.05	4.43	5.07	4.41	4.53
		LR04	5.02	4.98	4.63	4.84	5.08	4.55	5.08	4.75	4.74
	PLANKTONIC $\delta^{18}O$	ODP 646	4.42	4.77	4.70	4.04	4.50	4.57	4.70	3.66	4.27
		ODP 677	1.84	1.72	1.35	2.00	1.82	0.38	2.14	1.27	1.41
		ODP 806B	-1.12	-1.10	-1.17	-1.04	-0.44	-1.32	-0.99	-1.18	-1.24
		ODP 982	3.28	3.43	3.06	3.02	3.34	2.88	3.68	2.78	2.98
		ODP 1090	3.30	3.22	3.19	3.50	3.84	2.97	3.31	2.79	3.09
		ODP 1146	-0.83	-1.06	-1.04	-0.86	-0.63	-1.33	-0.60	-0.85	-0.73
		MD90-0963	-0.37	-0.46	-0.54	-0.49	-0.41	-0.98	-0.10	-0.66	-0.31
	SST (°C)	DSDP 607s	10.60	8.50	14.80	11.70	10.40	14.90	14.80	6.70	9.10
		DSDP 607w	4.50	4.70	8.80	5.40	5.80	8.40	7.90	0.40	4.10
		ODP 722	23.91	24.79	23.94	23.88	23.80	25.11	24.83	24.74	23.93
		ODP 806B	25.90	26.00	26.20	25.50	25.90	26.82	26.80	26.88	27.02
		ODP 846	20.50	22.10	20.70	20.10	20.70	20.60	21.20	21.80	20.10
		ODP 982	9.00	9.97	9.42	10.13	10.37	10.00	11.27	12.00	8.81
		ODP 1020	6.83	8.70	7.80	6.87	5.67	7.05	7.70	8.88	6.70
		ODP 1090	4.94	5.75	4.78	7.03	5.10	6.21	6.28	8.06	5.54
		ODP 1123	12.09	9.91	13.72	13.98	11.59	15.98	11.14	11.91	8.99
		ODP 1146	22.21	23.35	23.18	22.76	23.08	23.71	24.40	23.61	23.08
		MD97-2140	25.60	25.50	25.60	26.50	25.80	27.10	26.00	25.60	25.60
	BWT	DSDP 607	-1.00	-1.50	-1.40	-0.60	-0.70	0.20	-0.80	-0.30	-0.30
ICE		δD (‰)	-445	-440	-436	-442	-443	-438	-439	-441	-441
		CO_2 (ppmv)	182	190	195	201	199	190	189	184	188
		CH_4 (ppbv)	351	342	395	366	380	390	356	392	396
TERRESTRIAL	LOESS	MAR stacked	34.80	40.20	26.39	24.83	34.66	**	23.07	25.74	17.05
		MS stacked	0.19	0.12	0.09	0.04	0.09	0.18	0.08	0.03	0.07
		TP (%)	5.19	1.35	10.14	3.21	0.00	13.44	1.33	2.19	16.30
		Baikal (%)	2.10	1.80	4.60	3.20	3.20	5.20	3.00	3.30	4.20

** Stage not clearly resolved

Table 5. Maximum amplitude values for each termination. Termination amplitude is the difference between maximum glacial and interglacial values for each glacial-interglacial transition. The values are colour-coded according to strength, with deep purple being the greatest, and pale purple the weakest, termination amplitude for each record.

Termination			TI	TII	TIII	TIV	TV	TVI	TVII	TVIII	TIX
MARINE	BENTHIC $\delta^{18}O$	ODP 677	*	1.45	1.05	2.02	1.60	0.87	1.49	1.08	1.03
		ODP 1090	1.51	1.83	1.11	1.73	1.84	0.82	1.38	1.02	1.23
		ODP 1123	2.05	2.38	1.44	1.87	2.22	1.00	1.07	1.41	1.31
		ODP 1143	1.89	1.74	0.93	1.53	2.15	1.25	1.62	0.93	1.01
		ODP 1146	1.65	1.67	1.14	1.76	2.11	0.58	1.70	0.95	1.29
		ODP 846	1.61	1.90	0.80	1.50	1.94	0.41	1.31	0.61	1.02
		ODP 925	1.89	1.73	1.56	1.96	2.18	0.96	1.76	1.05	1.34
		ODP 980	2.38	2.27	1.61	2.07	2.50	1.74	1.99	1.46	1.81
		ODP 982	1.79	1.89	0.89	1.07	2.62	1.07	2.04	0.62	1.43
		ODP 983	1.96	2.06	1.34	1.78	1.81	0.83	1.57	1.41	1.65
		LR04	1.84	1.88	1.19	1.65	1.97	0.72	1.59	1.25	1.26
	PLANKTONIC $\delta^{18}O$	ODP 677	*	3.72	2.07	4.41	4.47	1.21	3.68	1.75	2.95
		ODP 806b	1.28	1.37	0.82	0.97	1.97	0.41	1.00	0.69	1.03
		ODP 982	2.00	2.49	1.23	1.63	1.59	1.03	2.14	0.95	1.39
		ODP 646	2.62	2.87	2.32	1.80	2.65	1.83	2.64	1.37	2.63
		ODP 1090	2.01	2.18	1.09	2.08	2.23	0.58	1.45	0.87	1.37
		ODP 1146	1.91	1.78	1.47	1.52	2.15	1.04	2.20	1.73	1.99
		MD90-0963	2.56	2.67	2.13	2.19	2.54	1.58	2.14	1.21	2.13
	SST (°C)	DSDP 607s	12.50	16.60	5.70	11.90	16.20	7.40	8.10	18.50	14.90
		DSDP 607w	11.70	12.70	5.00	11.00	13.70	6.80	8.20	17.80	12.70
		ODP 722	2.59	2.92	3.32	3.59	3.66	1.05	2.54	2.46	3.18
		ODP 806B	3.30	3.60	3.00	3.30	4.30	2.66	1.94	1.58	2.40
		ODP 846	2.70	3.00	3.10	3.70	3.30	2.60	2.30	1.90	3.60
		ODP 982	5.98	6.26	5.07	5.66	4.66	3.26	3.13	2.20	5.33
		ODP 1020	4.27	5.40	3.86	5.89	8.31	3.08	3.76	4.75	5.43
		ODP 1090	9.56	11.55	5.57	7.64	6.85	4.03	5.79	6.63	4.81
		ODP 1123	4.46	7.80	5.27	5.58	7.67	1.88	6.27	6.13	8.94
		ODP 1146	4.28	3.94	3.09	4.55	3.70	1.97	2.75	3.07	3.08
		MD97-2140	4.10	4.00	3.00	2.50	3.70	2.50	2.60	3.70	3.30
	BWT	DSDP 607	*	3.90	0.70	0.90	2.50	0.60	-0.10	0.70	2.20
ICE		δD (‰)	53	66	56	69	60	26	41	38	46
		CO_2 (ppmv)	103	97	85	98	90	58	71	56	72
		CH_4 (ppbv)	366	384	301	431	356	151	305	260	343
TERRESTRIAL	LOESS	MAR stacked	27.00	35.99	18.87	18.15	25.79	**	18.10	21.72	10.16
		MS stacked	0.56	0.62	0.46	0.67	0.56	0.75	0.25	0.25	0.19
		TP (%)	94.29	95.41	86.56	92.29	98.43	77.99	93.85	80.01	66.97
		Baikal (%)	*	41.30	27.70	39.80	42.80	21.00	40.80	38.80	30.30

*Top of core missing
** Stage not clearly resolved

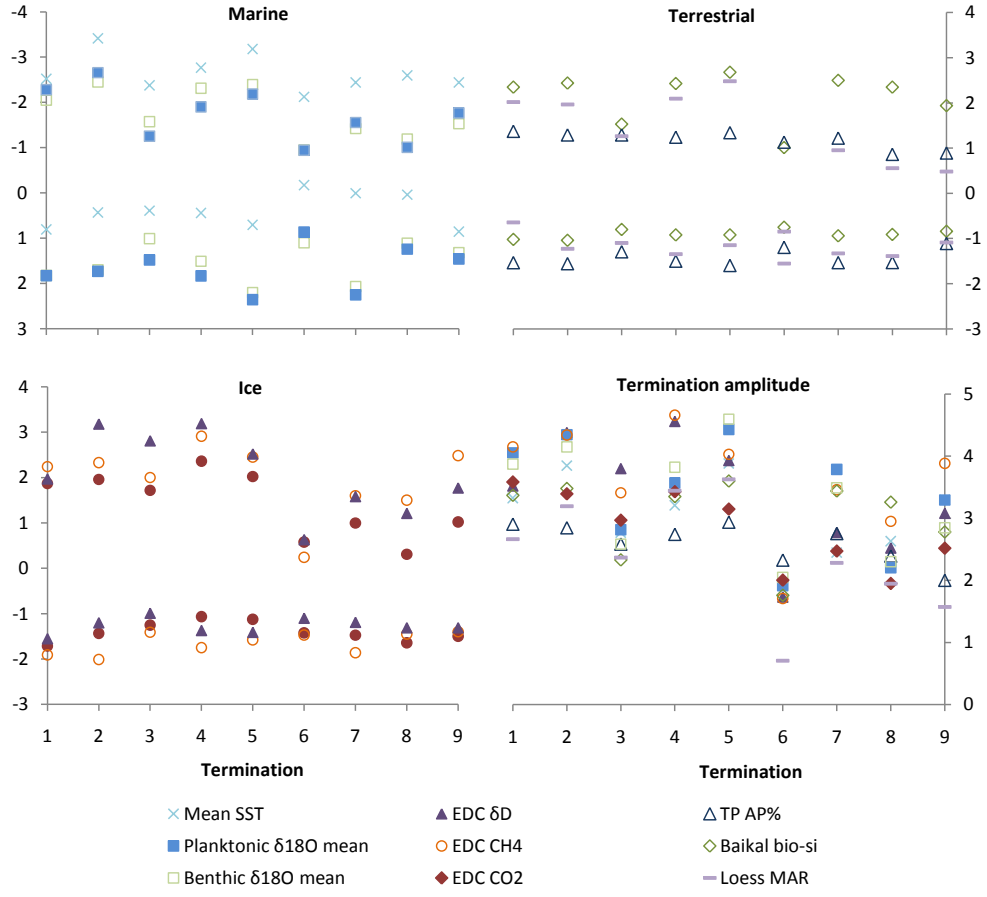

Fig. 4. Normalised peak values for each termination showing interglacial (upper series) and glacial maxima (lower series) and normalised termination amplitude. Each record's interglacial/glacial/termination amplitude values were normalised to the mean interglacial/glacial/termination amplitude value for that series.

little variability between glacials in the ice core data, at Lake Baikal and Tenaghi Philippon, and in loess MS. This suggests that when considering glacial variability, marine δ^{18}O, and to a lesser extent SST values, are more variable than other proxies.

3.1 The relative strength of interglacials

3.2 Increase in interglacial strength and termination amplitude following the Mid-Brunhes Event

The first and most obvious result seen in Table 3 is that there is a prevalence of strong interglacials since the Mid-Brunhes Event (MBE), i.e. from MIS11 to MIS1, in almost all δ^{18}O and SST records and Tenaghi Philippon, thus confirming the impression derived from the ice core record (EPICA, 2004). However this is not uniformly true; MIS 7 (specifically event 7.5) is typically no stronger than MIS 15 or MIS 19 in almost all records, while the Holocene is rather subdued in the SST records. Although this calls into question the idea that there was a step change from strong to weak interglacials at the MBE (EPICA, 2004), it is nonetheless true that across most of the records four of the last five interglacials were the strongest of the last nine. One reason for the cooler interglacials of the earlier period is of course the weaker forcing due to the lower interglacial CO_2 concentrations that are observed. This observation provides a mechanism that would explain a common pattern of relative interglacial warmth globally, in contrast to what we might expect under direct astronomical control. However, it also highlights the fact that we cannot yet diagnose a cause for the lower CO_2 in these interglacials.

The Asian terrestrial records somewhat vary from this general trend; two of the strongest interglacials in the MAR record occur before the MBE, and magnetic susceptibility is particularly high in MIS 13. In the case of loess accumulation, this may be partly a result of the chosen index: MAR is very low in interglacials, with little variation between interglacials, and it is not clear that relative interglacial strength is properly represented in the residual values. While the MS record fits the general pattern with the three weakest interglacials occuring pre-MBE, the strongest signal is seen in

MIS 13; this has been suggested to indicate a strong East Asian summer monsoon (Guo et al., 2009) at this time. Lake Baikal also shows some differences from the general pattern, with MIS15 showing particular relative strength. This stage is also relatively strong in the planktonic record from ODP1146 in the South China Sea. Although this record is quite noisy, which counsels caution in interpreting narrow maxima, the common strength of MIS15 in this record and Lake Baikal perhaps suggests that the strength of this interglacial stage in Asia is a robust feature of the data. MIS19 is unexpectedly strong in the EDC ice core methane record, and in site 646 (south of Greenland) planktonic δ^{18}O.

Within the SST records there is some regional variability in the increase in interglacial strength (Fig. 5). While there is a relatively small increase in interglacial strength in tropical SSTs, at higher latitudes the increase from pre- to post-MBE interglacials is more obvious. It must be noted that the alkenone temperature proxy reaches saturation at around 28 °C and therefore in warmer locations may underestimate interglacial warmth (and therefore termination amplitude) in warmer interglacials such as MIS 5 and 11.

Outstanding interglacials

The strongest interglacial in the marine records is typically MIS 5 (actually in four benthic, five SST and three planktonic records, as well as in the LR04 stack). Stage 11 is the strongest interglacial in one planktonic record, three SST records, three benthic datasets, and at Lake Baikal. MIS 9 is the strongest interglacial in deuterium, CO_2 and CH_4, from Antarctic ice and in two benthic datasets, and two SST records. The strength of the methane signal is particularly surprising since methane is considered a mainly northern hemisphere and/or tropical signal, while most of the other parameters are related to Antarctica and the Southern Ocean. The peak in methane is rather narrow and sharp, and one possibility is that it is missing from other records due to lower time resolution.

While the pattern of strong events is apparent in Table 3, caution is needed, since the oxygen isotope records are all, to some extent, driven by the same underlying signal of global ice volume. Nonetheless, we note that MIS11 is the strongest interglacial in SST records from the North Atlantic (607) and equatorial Pacific (806B) as well as being among the strongest in more southern records (1123 SST, EDC CO_2). MIS 5 is the strongest record in SSTs from a North Atlantic site (982), a North Pacific site (1020), two equatorial sites (722, 846) and a South Atlantic site (1090), as well as in Antarctic temperature. This confirms that within the present datasets there do appear to be some individual interglacials that are globally stronger than others, although further terrestrial data are certainly needed before this conclusion can be confirmed and regional patterns can be identified. This is an interesting result, because recent speculation about the role of the bipolar seesaw in inducing early interglacial warmth

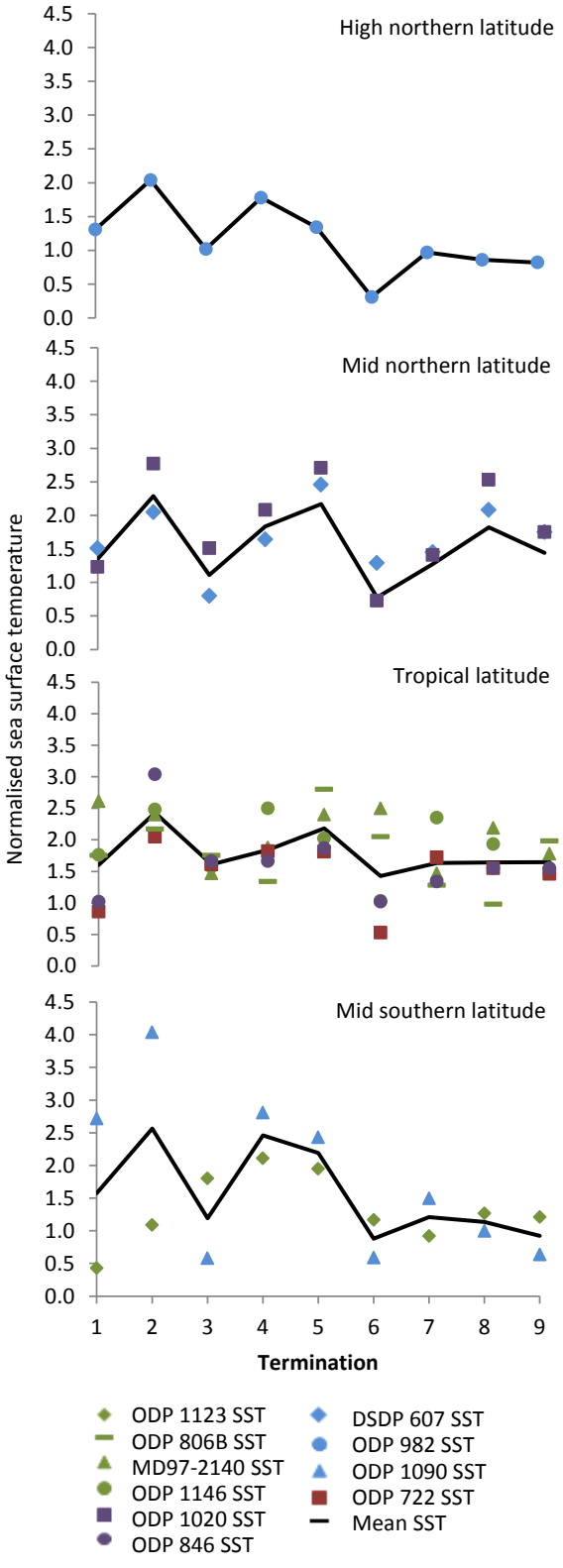

Fig. 5. Normalised peak interglacial values for sea surface temperature (SST) grouped by latitude with mean SST values for each group.

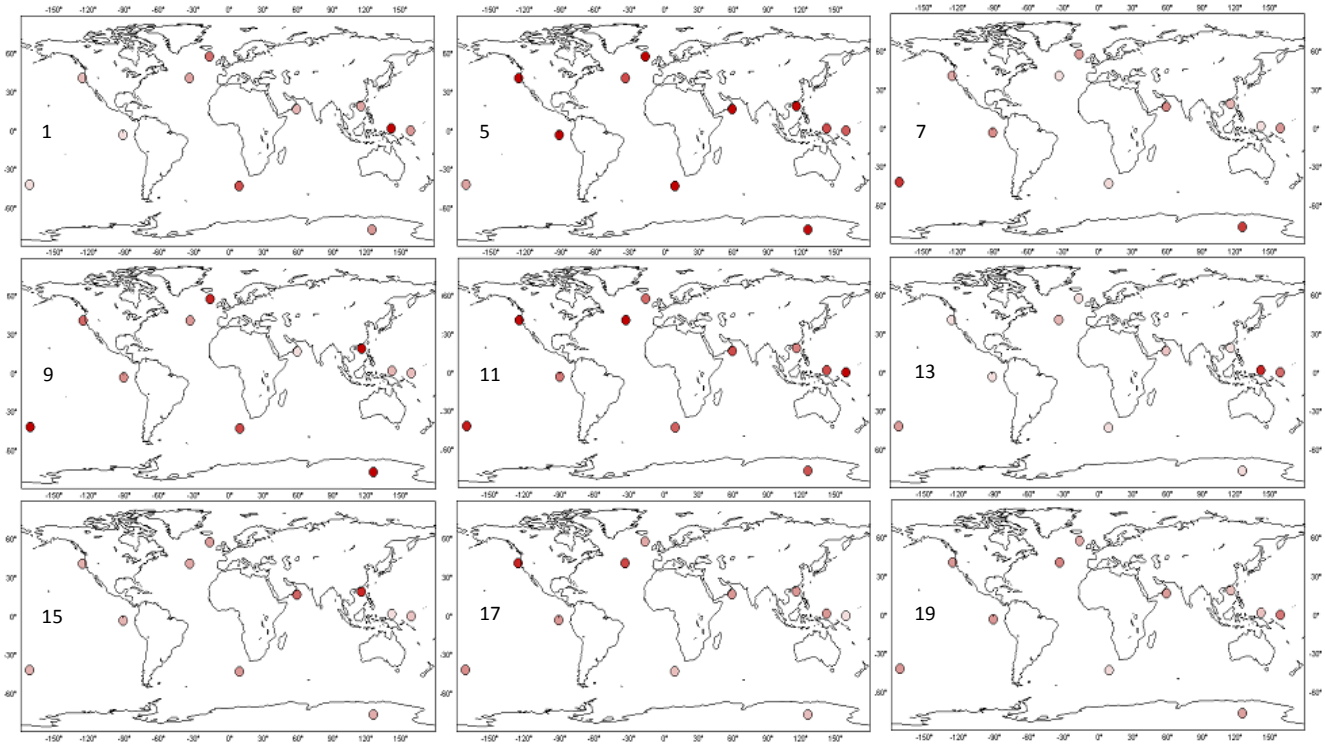

Fig. 6. Maps of peak interglacial sea surface temperature (SST) and EDC temperature for MIS 1-19. In the colour scale, the darkest red reflects the highest SST and the lightest the lowest SST.

in Antarctica (Masson-Delmotte et al., 2010; Holden et al., 2009) might have led us to expect regional differences in which interglacials were warmest. It remains quite possible that the timing of peak warmth within an interglacial is not synchronous in different records, but this result nonetheless suggests that, even if peak southern interglacial warmth is controlled by the bipolar seesaw mechanism, it nonetheless occurs in the context of an interglacial that experiences global warmth.

The weakest interglacial in the majority of marine records, in Antarctic δD and methane, and at Baikal, is MIS 13. There are however two interesting exceptions to this finding. Firstly, the stacked MS signal for loess is strongest in this stage, and it has been suggested that there was generally a strong summer monsoon in this period (Guo et al., 2009). SSTs at western equatorial Pacific sites 806B and MD97-2140 are also elevated in this stage in contrast to other SST records. Additionally, it was recently shown (de Vernal and Hillaire-Marcel, 2008) that large amounts of pollen were present in a marine core from off south Greenland during the second half of MIS13 (more than in any interglacial except for MIS11), suggesting a reduced Greenland ice sheet. This is despite the fact that both summer and winter SST estimated from dinocyst assemblages for the same core were relatively low compared to (for example) MIS 5. We can speculate (but without strong observational or modelling evidence) that the prolonged period without a deep glacial from MIS 15 to 13 allowed shrinkage of the ice sheet in this region of Greenland during the later parts of MIS 13. Despite the exceptions, MIS 13 is clearly the weakest interglacial of the last 800 ka globally.

We note, as have previous authors working only with the marine isotopic profiles (Yin and Berger, 2010), that there is no clear relationship between astronomical parameters and the relative strength of each interglacial. Obliquity is stronger in the second half of the last 800 ka, but strong interglacials are associated with both strong precessional forcing (MIS 5) and very weak precessional forcing (MIS 11).

Figure 6 shows maps of relative interglacial strength for peak SST and Antarctic temperature (deuterium) for each interglacial. The patterns they display should serve as modelling targets for those attempting to model the climate during contrasting interglacials. They also highlight the near global pattern of strength of MIS 5 and 11, and weakness of, for example, MIS 13.

3.3 The relative strength of glacials

Table 4, showing the relative strength of glacials (specifically of the period immediately before the termination, which is typically the coldest phase of the glacial), shows an interesting mirror of the pattern seen in the interglacials (Table 3): strong glacials (in dark blue) are found predominantly on the left hand side of the table, occuring since (and including)

MIS 12. However within this overall pattern stages 8 and 16 stand out; MIS 8 appears to be a weak glacial in many records, particularly benthic $\delta^{18}O$, pre-empting the weak interglacial stage 7. We should qualify this statement for some records however: the part of MIS 8 immediately preceding the termination is what is represented here; however looking for example at the ice core records, stronger glacial values are found in an earlier dip at about 270 ka ago, some 15–20 ka before the pre-termination minimum. MIS16 is a particularly strong glacial in both planktonic and benthic $\delta^{18}O$, and to some extent CH_4. However, it is rather weak in SST records. This is therefore one of the cases where the perception from isotopic records – that MIS16 is a strong glacial – does not seem to hold for other datasets. This could perhaps indicate that the isotopic strength of MIS16 is more of an ice volume than a climate signal.

MIS 12 and 16 appear as the strongest glacials in most benthic and planktonic isotopic records. There is no one glacial that stands out as the coldest in SST however; MIS 2 is on average the coolest but not significantly so. MIS 2 is particularly strong in Dome C deuterium and in CO_2: however, note that CO_2 concentrations lower than those seen in MIS 2 occur in earlier parts of MIS 16 and MIS 18, but not just before the terminations. It has been suggested (Lüthi et al., 2008) that CO_2 concentrations are generally offset to lower values (in both glacials and interglacials) between 650 and 750 ka ago. MIS 14 is particularly weak in a range of records; indeed in many planktonic records, in Chinese loess and at Tenaghi Philippon it is sufficiently weak that one could question its designation as a glacial.

There is some suggestion that a particularly strong (weak) glacial maximum is indicative of a strong (weak) post-termination interglacial peak. This pattern can be seen most clearly in the symmetric patterns of the interglacial and glacial average data from marine $\delta^{18}O$ records (Fig. 4a). Clearly, glacial strength does not quantitatively dictate the strength of the following interglacial. In particular, the very strong (isotopically) MIS 16, is followed by a MIS 15 which, although stronger (in both marine isotopic and ice core parameters) than the adjacent interglacials (MIS 13, 17), is considerably weaker than many later interglacials. Nonetheless it is interesting to consider the implications of the apparent "rule" that a strong glacial maximum (in isotopic terms, perhaps resulting from particularly large northern ice sheets) leads to an interglacial that is strong within the context of its adjacent interglacials. Since the glacials precede the respective interglacials, this suggests that the strength of the interglacial may already have been partially determined before the termination, so that the failure to find a relationship between interglacial strength and the immediate astronomical forcing is unsurprising. One possible cause for the apparent relationship between glacial and interglacial strength is suggested by the conceptual model of Parrenin and Paillard (2003). In their model, terminations occur when a combination of ice sheet volume and astronomical forcing reach a threshold, which implies that, for a termination to occur during periods of weak forcing, a stronger glacial maximum is required. On the other hand glaciation is initiated only as a function of astronomical forcing, implying a tendency for a longer period of deglaciation when forcing is weak; this gives the potential, despite starting from a larger ice sheet, for a greater level of deglaciation, and a stronger isotopic interglacial, at times of weak forcing. In this view it is therefore (paradoxically) weak astronomical forcing which tends to lead to strong glacial cycles (both to stronger glacial maxima and greater deglaciation, i.e. stronger interglacials), although the relationship between glacial and interglacial strength should be complex

3.4 The relative amplitude of terminations

As with interglacial peak, and as expected from the partial symmetry of glacial and interglacial strength in many records, termination amplitude is typically greater for the last five terminations (Table 5, Fig. 4d) – TI to TV – than the previous four – TVI to TIX. Amplitude is on average 40–45% higher in benthic and planktonic $\delta^{18}O$, CO_2 and CH_4. Again TVII somewhat breaks the pattern, being of high amplitude in many records, mainly because of the exceptional strength of glacial MIS 16, while TIII is of lower amplitude than the surrounding ones.

3.5 Intra-interglacial strength and trends: case studies

While the compilation seen in Fig. 2 allows an overview of the entire record, the indexing in Tables 3–5 concentrates on the periods just before and after terminations. While these often represent the glacial minimum and interglacial maximum, they do not reveal the full complexity of the climate records involved. In particular we have situations in which the maximum identified in one record is asynchronous with the maximum in another, but this will not be identified in the work of the previous parts of Sect. 3. In this sub-section we concentrate on interglacials and use case studies to illustrate the type of complexity that will have to be confronted in future work.

3.5.1 Marine isotope stage 7

MIS 7 represents an interesting interglacial in which there are three peaks, of which the first (sub-stage 7e, containing the isotopic event 7.5), generally considered as the full interglacial, is relatively weak in many records, but the two subsequent stages (7c, 7a) also exhibit full interglacial characteristics in some records. To illustrate this we present the entirety of MIS 7 on an expanded age scale in a range of records (Fig. 7).

The full range of behaviours is observed in the different records. In EPICA Dome C deuterium and CO_2, sub-stages MIS 7c and 7a show levels distinctly lower than those of 7e, but nonetheless comparable to those observed at any part of

interglacial stages 13 and 15. Sub-stages 7a and 7c are more clearly resolved in planktonic δ^{18}O than in benthic records, and are of comparable strength to MIS 7e; however in six of the 17 δ^{18}O records a stronger signal is seen in stage 7c than 7e. There is a well-resolved peak for each of the sub-stages in Lake Baikal BioSi%, and the strongest peak is found in 7c; if this had been taken as the true interglacial at Baikal, then MIS 7 at Baikal would be seen as stronger than MIS 19. Similarly well-resolved multiple interglacial peaks are also seen in the planktonic MD90-0963 record.

The implications of this complexity are: (a) while glacial conditions may have been experienced at a few sites during marine isotope sub-stage 7b, many sites experienced 7c–7a as an almost continuous period of relatively strong interglacial conditions and (b) on the other hand MIS 7e and 7c are separated by a period with conditions that are close to fully glacial in almost all respects (and certainly as strongly glacial as MIS 14), (c) MIS 7c has at least as much interglacial character as MIS 13 and 15. In fact there seems no clear reason (other than a prior assumption that interglacials do not recur so frequently) from the records presented here not to define MIS 7c (or the period MIS 7c to 7a) as an interglacial separate from MIS 7e.

3.5.2 MIS 13 and 15

The interglacial peak after Termination VI corresponds to marine isotope event 13.3, however in many records including ice core deuterium and methane, Baikal, and most of the benthic records (including LR04), more strongly interglacial values are seen in the later part of MIS 13 corresponding with event 13.1, than at 13.3 (Fig. 7). Marine isotopic event 13.1 is some 20 ka later than 13.3, so it is not clear whether the whole stage should be considered as a very long but weak interglacial, or as two interglacials separated by a very weak cooling. As has recently been pointed out (Yin and Berger, 2010) event 13.1 also has contains two separate peaks in many records, the typically stronger sub-event 13.11 and weaker 13.13. As can be seen from Figs. 2 and 7, there are a variety of behaviours for this event: as an example, the CO_2 and CH_4 records show a sequence of peaks of different strengths. However, across the records, our synchronisation is not sufficiently precise to align events at such detail with confidence, and we leave this for a later iteration.

MIS 15 also shows a complex structure, and the interpretation of which is the strongest section is less clear than for MIS 13; in most records peaks of comparable magnitude are seen in sub-stages 15e and 15a, while 15c is not clearly differentiated from 15a in some records, and lacking entirely in Baikal. It is difficult to discuss the sub-stages of MIS 13 and 15 with any confidence in the SST records, emphasising the need for improved resolution of datasets in this region. As a final comment we note that the whole section from the start of MIS 15 to the end of MIS 13 is of low amplitude in many records. MIS 14 is barely more prominent in many records

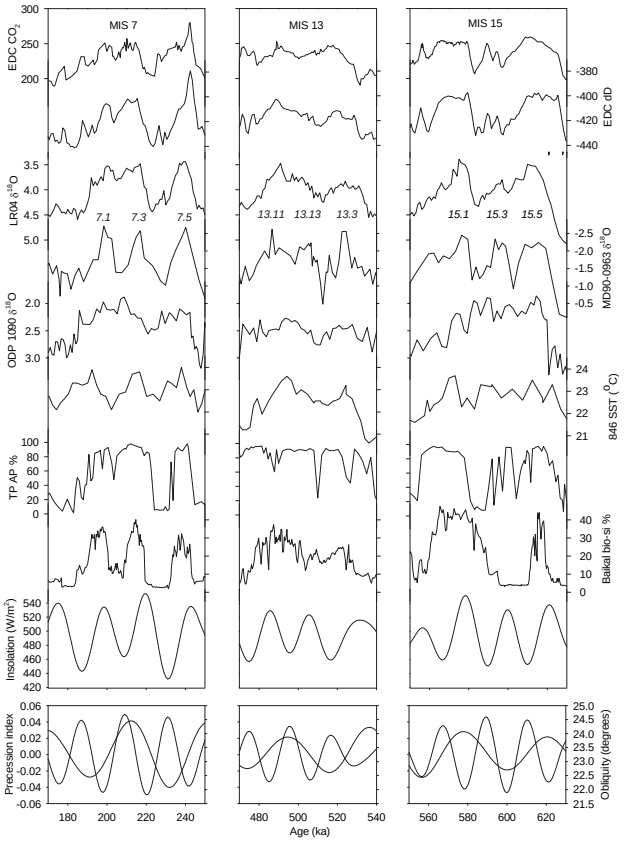

Fig. 7. Interglacial stages 7, 13 and 15 showing multiple interglacial peaks in selected records. Sub-stages are given in italics.

than the section between the two major peaks of MIS 15. We should therefore be cautious to ensure that our labelling of a long period as "glacial" or "interglacial" does not lead us to ignore significant climatic transitions.

3.6 Shapes and trends in interglacials

It is beyond the scope of this paper to look in detail at the shape of each interglacial. Furthermore it would be inappropriate to look in detail at recent interglacials such as MIS 5 using only the limited dataset here since many more datasets with greater resolution are available for recent periods. However we can make a few preliminary observations about contrasts in shape between different records and different interglacials (Fig. 8). Taking Dome C deuterium as an example, the beginning of interglacial stages 5, 7, 9, and 19 (immediately after the glacial termination) show a clear structure with the highest values at the start of the stage in a rather sharp peak; on the other hand in MIS 11 values increase more gradually as the interglacial progresses to a later peak, while in MIS 15 values rise sharply and then remain fairly constant, with a flat profile. CO_2 shows many similarities to deuterium, though there are also differences for example,

the flatter profile of MIS 5 after its initial peak (event 5.5), and in the earlier part of MIS 11. Benthic isotopes do not obviously show the same pattern; in LR04 early interglacial peaks are absent, and values typically taper to a later interglacial maximum. MIS 11 is more symmetrical in profile than in δD, indeed we would have to be cautious in deciding which part of the ice core δD should be aligned with the peak in LR04 within this stage. Again, more detailed analysis of these points is required because the relatively low resolution of some records, and the smoothing inherent in the stacked LR04 record, may be giving a false impression of these features. Further study will be required to assess the detailed alignment within each interglacial, and the significance of the contrasting shapes observed.

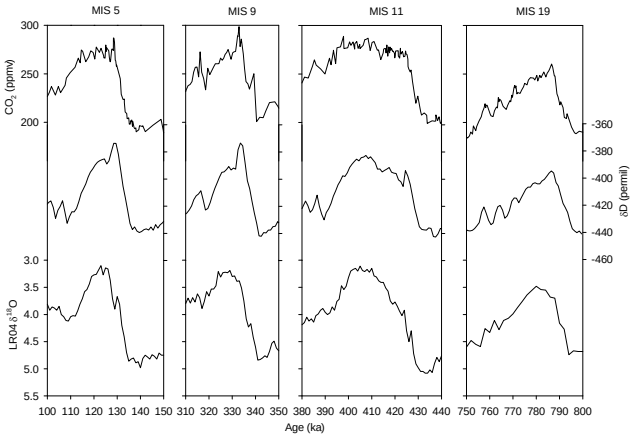

Fig. 8. Interglacial stages 5, 9, 11, and 19 showing variation in shape and trend between records.

4 Conclusions

The kind of compilation we have made here is simplified by the fact that so few records meet our criteria. However, one consequence of that is that it is very hard to make statements about the global pattern of change and of glacial and interglacial strength based on such sparse geographic coverage. The deep ocean is reasonably well-represented by isotopic records, and the different benthic records show relatively little variability between them in terms of amplitude, even if there are phase differences between them. The surface ocean, represented by 10 suitable SST records, shows greater variability than in the isotopic records; regional differences between tropical and higher latitudes can be tentatively identified. Specific proxy measurements of bottom water temperature are limited; some extend so far only to around 500 ka (Elderfield et al., 2010), and we are completely lacking data from the African, American and Australian continents. Thus while our datasets do represent very significant components of the Earth system including CO_2 (representing both a range of ocean processes and a significant climate forcing) and the deep ocean isotopes (representing at least in part global ice volume) and surface temperatures, we have to recognise that significant regional effects could still be unnoticed in this compilation.

Nevertheless we have been able to form some tentative conclusions based on the data that are available. Firstly there is a very wide range of interglacial (and glacial) behaviour, and it is probably not helpful to think of a single interglacial-glacial cycle "type" that has to be understood. The impression (formed until now mainly from benthic isotope and Antarctic ice core data) that the last 450 ka experienced much stronger amplitude interglacials than did the preceding 350 ka is generally confirmed, and seems to apply to records representing a wide range of regions. There is however one clear exception (the weak MIS 7), which suggests that the conditions under which a weak cycle can occur had not completely changed following the MBE, but perhaps only that the probability for a weak cycle had been reduced.

It appears that the strength of a glacial may influence the strength of the following interglacial with interesting implications for the memory and predictability of the system, and for the role of astronomical forcing in determining the strength (as opposed to the timing) of an interglacial.

Finally we note that several of the periods we traditionally think of as interglacial actually consist of complex structures, including in some cases multiple peaks separated by periods of significant "glacial" strength. In considering the causes and strengths of glacial-interglacial transitions, it is therefore important not to be influenced by the nomenclature into considering only a subset of the available events.

Collection of datasets to fill the gaps in this work should be an important priority for the palaeoceanographic and terrestrial communities; work is currently underway to recover continental palaeoclimate records from various sites through the International Continental Scientific Drilling Program (ICDP), for example Lakes Malawi and Bosumtwi in Africa, Asian lakes El'gygytgyn and Qinghai, Lakes Petén Itzá and Potrok Aike in the Americas, and the Dead Sea.

Further work is clearly needed to make more detailed compilations for specific glacial and interglacial periods. Such work will not be able to ignore the major synchronisation issues that our broad investigation has avoided. However many more records of shorter length, or which are incomplete, will be able to be used. One obvious target will be periods that have similar astronomical forcings but different climate responses, recognising that no two periods have identical forcing. Finally we hope that modelling exercises focussed on this period, or on specific interglacials, will be encouraged by the possibility of making at least qualitative data-model comparisons.

Supplementary material related to this article is available online at: http://www.clim-past.net/7/361/2011/ cp-7-361-2011-supplement.zip.

Acknowledgements. This study is part of the British Antarctic Survey Polar Science for Planet Earth Programme, and the QUEST-DESIRE project (grant NE/E007600/1). It was funded by the Natural Environment Research Council. We would like to thank Simon Crowhurst, Lorraine Lisiecki, and Regine Röthlisberger for their advice and assistance, and Anne de Vernal, Torsten Bickert, Ian Hall, Kira Lawrence, Alfredo Martínez Garcia, Sindia Sosdian, Youbin Sun, and Chronis Tzedakis for providing data. We thank Michel Crucifix and Chronis Tzedakis for their very helpful reviews, and their precise editing suggestions.

Edited by: L. Skinner

References

Aksu, A. E., de Vernal, A., and Mudie, P. J.: High-resolution foraminiferal, palynological and stable isotopic records of upper Pleistocene sediments from Labrador Sea: paleoclimatic and paleoceanographic trends, Proc. ODP Sci. Res., 105B, 617–652, 1989.

Bassinot, F., Labeyrie, L., Vincent, E., Quidelleur, X., Shackleton, N. J. and Lancelot, Y.: The astronomical theory of climate and the age of the Brunhes-Matuyama magnetic reversal, Earth Planet. Sc. Lett., 126, 91–108, Data archived at the World Data Center for Paleoclimatology, Boulder, Colorado, USA, 1994.

Berger, A. L. and Loutre, M.-F.: Insolation values for the climate of the last 10 million years, Quaternary Sci. Rev., 10, 297–317, 1991.

Bickert, T., Curry, W. B., and Wefer, G.: Late Pliocene to Holocene (2.6–0 Ma) Western Equatorial Atlantic deep-water circulation: inferences from benthic stable isotopes, Proc. ODP Sci. Res., 154, 239–254, 1997.

Bloemendal, J., Liu, X., Sun, Y., and Li, N.: An assessment of magnetic and geochemical indicators of weathering and pedogenesis at two contrasting sites on the Chinese Loess plateau, Palaeogeogr. Palaeocl. Palaeoecol., 257, 152–168, 2008.

Clemens, S. C. and Prell, W. L.: Data report: Oxygen and carbon isotopes from site 1146, northern South China Sea, Proc. ODP Sci. Res., 184, chapter 3, 2003.

Crundwell, M., Scott, G., Naish, T., and Carter, L.: Glacial-interglacial ocean climate variability from planktonic foraminifera during the Mid-Pleistocene transition in the temperate Southwest Pacific, ODP Site 1123, Palaeogeogr. Palaeocl. Palaeoecol., 260, 202–229, 2008.

de Garidel-Thoron, T., Rosenthal, Y., Bassinot, F., and Beaufort, L.: Stable sea surface temperatures in the western Pacific warm pool over the past 1.75 million years, Nature, 433, 294–298, Data archived at the World Data Center for Paleoclimatology, Boulder, Colorado, USA, 2005.

de Vernal, A. and Hillaire-Marcel, C.: Natural variability of Greenland climate, vegetation, and ice volume during the past million years, Science, 320, 1622–1625, 2008.

Elderfield, H., Greaves, M., Barker, S., Hall, I. R., Tripati, A., Ferretti, P., Crowhurst, S., Booth, L., and Daunt, C.: A record of bottom water temperature and seawater δ^{18}O for the Southern Ocean over the past 440 kyr based on Mg/Ca of benthic for a mini feral *Uvigerina* spp., Quaternary Sci. Rev., 29, 160–169, 2010.

EPICA: Eight glacial cycles from an Antarctic ice core, Nature, 429, 623–628, 2004.

Ganopolski, A. and Calov, R.: Simulation of glacial cycles and abrupt climate changes with a climate-ice sheet model of intermediate complexity, Geophys. Res. Abst., 10, EGU2008-A-01425, 2008.

Guo, Z. T., Berger, A., Yin, Q. Z., and Qin, L.: Strong asymmetry of hemispheric climates during MIS-13 inferred from correlating China loess and Antarctica ice records, Clim. Past, 5, 21–31, doi:10.5194/cp-5-21-2009, 2009.

Hall, I. R., McCave, I. N., Shackleton, N. J., Weedon, G., and Harris, S. E.: Intensified deep Pacific inflow and ventilation in Pleistocene glacial times, Science, 412, 809–812, 2001.

Herbert, T. D., Peterson, L. C., Lawrence, K. T., and Liu, Z.: Tropical Ocean Temperatures Over the Past 3.5 Million Years, Science, 328, 1530–1534, Data archived at the World Data Center for Paleoclimatology, Boulder, Colorado, USA, 2010.

Herbert, T. D., Schuffert, J. D., Andreasen, D., Heusser, L., Lyle, M., Mix, A. C., Ravelo, A. C., Stott, L. D., and Herguera, J. C.: Collapse of the California current during glacial maxima linked to climate change on land, Science, 293, 71–76, Data archived at the World Data Center for Paleoclimatology, Boulder, Colorado, USA, 2001.

Hodell, D. A., Charles, C. D., Curtis, J. H., Nortyn, P. G., Ninnemann, U. S., and Venz, K. A.: Data report: Oxygen isotope stratigraphy of ODP leg 177 sites 1088, 1089, 1090, 1093, and 1094, Proc. ODP Sci. Res., 177, 1–26, 2003.

Holden, P. B., Edwards, N. R., Wolff, E. W., Lang, N. J., Singarayer, J. S., Valdes, P. J., and Stocker, T. F.: Interhemispheric coupling, the West Antarctic Ice Sheet and warm Antarctic interglacials, Clim. Past, 6, 431–443, doi:10.5194/cp-6-431-2010, 2010.

Hooghiemstra, H., Melice, J. L., Berger, A. L., and Shackleton, N. J.: Frequency spectra and paleoclimatic variability of the high-resolution 30–1450 ka Funza I pollen record (Eastern Cordillera, Colombia), Quaternary Sci. Rev., 12, 141–156, 1993.

Imbrie, J., Berger, A., Boyle, E. A., Clemens, S. C., Duffy, A., Howard, W. R., Kukla, G., Kutzbach, J., Martinson, D. G., McIntyre, A., Mix, A. C., Molfino, B., Morley, J. J., Peterson, L. C., Pisias, N. G., Prell, W. L., Raymo, M. E., Shackleton, N. J., and Toggweiler, J. R.: On the structure and origin of major glaciation cycles. 2. the 100 000-year cycle, Paleoceanography, 8(6), 699–735, 1993.

Imbrie, J. and Imbrie, J. Z.: Modeling the climatic response to orbital variations, Science, 207, 943–953, 1980.

Jouzel, J., Alley, R. B., Cuffey, K. M., Dansgaard, W., Grootes, P., Hoffmann, G., Johnsen, S. J., Koster, R. D., Peel, D., Shuman, C. A., Stievenard, M., Stuiver, M., and White, J.: Validity of the temperature reconstruction from water isotopes in ice cores, J. Geophys. Res., 102(C12), 26471–26487, 1997.

Jouzel, J., Masson-Delmotte, V., Cattani, O., Dreyfus, G., Falourd, S., Hoffmann, G., Minster, B., Nouet, J., Barnola, J. M., Chappellaz, J., Fischer, H., Gallet, J. C., Johnsen, S., Leuenberger, M., Loulergue, L., Luethi, D., Oerter, H., Parrenin, F., Raisbeck, G.,

Raynaud, D., Schilt, A., Schwander, J., Selmo, E., Souchez, R., Spahni, R., Stauffer, B., Steffensen, J. P., Stenni, B., Stocker, T. F., Tison, J. L., Werner, M., and Wolff, E. W.: Climate variability over the past 800 000 years, Science, 317, 793, Data archived at the World Data Center for Paleoclimatology, Boulder, Colorado, USA, 2007.

Kawamura, K., Parrenin, F., Lisiecki, L., Uemura, R., Vimeux, F., Severinghaus, J. P., Hutterli, M. A., Nakazawa, T., Aoki, S., Jouzel, J., Raymo, M. E., Matsumoto, K., Nakata, H., Motoyama, H., Fujita, S., Goto-Azuma, K., Fujii, Y., and Watanabe, O.: Northern Hemisphere forcing of climatic cycles in Antarctica over the past 360 000 years, Nature, 448(7156), 912–U4, 2007.

Kohfeld, K. E. and Harrison, S. P.: Glacial-interglacial changes in dust deposition on the Chinese Loess Plateau, Quaternary Sci. Rev., 22, 1859–1878, 2003.

Laskar, J., Robutel, P., Joutel, F., Gastineau, M., Correia, A. C. M., and Levrard, B.: A long-term numerical solution of the insolation quantities of the Earth, Astron. Astrophys., 428, 261–285, 2004.

Lawrence, K. T., Herbert, T. D., Brown, C. M., Raymo, M. E., and Haywood, A. M.: High-amplitude variations in North Atlantic sea surface temperature during the Pliocene warm period, Paleoceanography, 24, PA2218, Data archived at the World Data Center for Paleoclimatology, Boulder, Colorado, USA, 2009.

Lisiecki, L. E. and Lisiecki, P. A.: Application of dynamic programming to the correlation of paleoclimate records, Paleoceanography, 17(4), 1049, doi:10.1029/2001PA000733, 2002.

Lisiecki, L. E. and Raymo, M. E.: A Pliocene-Pleistocene stack of 57 globally distributed benthic δ^{18}O records, Paleoceanography, 20, PA1003, Data archived at the World Data Center for Paleoclimatology, Boulder, Colorado, USA, 2005.

Lisiecki, L. and Raymo, M. E.: Atlantic overturning responses to Late Pleistocene climate forcings, Nature, 456, 85–88, 2008.

Lisiecki, L. E. and Raymo, M. E.: Diachronous benthic delta δ^{18}O responses during late Pleistocene terminations, Paleoceanography, 24, PA3210, doi:10.1029/2009PA001732, 2009.

Liu, Z. and Herbert, T. D.: High-latitude influence on the eastern equatorial Pacific climate in the early Pleistocene epoch, Nature, 427, 720–724, Data archived at the World Data Center for Paleoclimatology, Boulder, Colorado, USA, 2004.

Loulergue, L., Schilt, A., Spahni, R., Masson-Delmotte, V., Blunier, T., Lemieux, B., Barnola, J. M., Raynaud, D., Stocker, T. F., and Chappellaz, J.: Orbital and millenial-scale features of atmospheric CH_4 over the past 800 000 years, Nature, 453, 383–386 Data archived at the World Data Center for Paleoclimatology, Boulder, Colorado, USA, 2008.

Lüthi, D., Le Floch, M., Bereiter, B., Blunier, T., Barnola, J. M., Siegenthaler, U., Raynaud, D., Jouzel, J., Fischer, H., Kawamura, K., and Stocker, T. F.: High-resolution carbon dioxide concentration record 650 000–800 000 years before present, Nature, 453, 379–382, Data archived at the World Data Center for Paleoclimatology, Boulder, Colorado, USA, 2008.

Magri, D. and Tzedakis, P. C.: Orbital signatures and long-term vegetation patterns in the Mediterranean, Quatern. Int., 73/74, 69–78, 2000.

Martinez-Garcia, A., Rosell-Mele, A., Geibert, W., Gersonde, R., Masque, P., Gaspari, V., and Barbante, C.: Links between iron supply, marine productivity, sea surface temperature, and CO_2 over the last 1.1 Ma, Paleoceanography, 24, PA1207, doi:10.1029/2008PA001657, 2009.

Masson-Delmotte, V., Stenni, B., Pol, K., Braconnot, P., Cattani, O., Falourd, S., Kageyama, M., Jouzel, J., Landais, A., Minster, B., Barnola, J. M., Chappellaz, J., Krinner, G., Johnsen, S., Rothlisberger, R., Hansen, J., Mikolajewicz, U., and Otto-Bliesner, B.: EPICA Dome C record of glacial and interglacial intensities, Quaternary Sci. Rev., 29, 113–128, 2010.

Medina Elizalde, M. and Lea, D.: The Mid-Pleistocene Transition in the Tropical Pacific, Science, 310, 1009–1114, Data archived at the World Data Center for Paleoclimatology, Boulder, Colorado, USA, 2005.

Mix, A. C., Le, J., and Shackleton, N. J.: Benthic foraminiferal stable isotope stratigraphy of site 846, 0–1.8 Ma, Proc. ODP Sci. Res., 138, 839–854, Data archived at the World Data Center for Paleoclimatology, Boulder, Colorado, USA, 1995.

Mudelsee, M.: Ramp function regression: a tool for quantifying climate transitions, Comput. Geosci., 26, 293–307, 2000.

Mudelsee, M. and Schulz, M.: The mid-Pleistocene climate transition: onset of 100 ka cycle lags ice volume build-up by 280 ka, Earth Planet. Sc. Lett., 151, 117–123, 1997.

Oliver, K. I. C., Hoogakker, B. A. A., Crowhurst, S., Henderson, G. M., Rickaby, R. E. M., Edwards, N. R., and Elderfield, H.: A synthesis of marine sediment core δ^{13}C data over the last 150 000 years, Clim. Past, 6, 645–673, doi:10.5194/cp-6-645-2010, 2010.

Paillard, D., Labeyrie, L., and Yiou, P.: Macintosh program performs time-series analysis, Eos Trans. AGU, 77, 379, 1996.

Parrenin, F. and Paillard, D.: Amplitude and phase of glacial cycles from a conceptual model, Earth Planet. Sc. Lett., 214, 243–250, 2003.

Parrenin, F., Barnola, J.-M., Beer, J., Blunier, T., Castellano, E., Chappellaz, J., Dreyfus, G., Fischer, H., Fujita, S., Jouzel, J., Kawamura, K., Lemieux-Dudon, B., Loulergue, L., Masson-Delmotte, V., Narcisi, B., Petit, J.-R., Raisbeck, G., Raynaud, D., Ruth, U., Schwander, J., Severi, M., Spahni, R., Steffensen, J. P., Svensson, A., Udisti, R., Waelbroeck, C., and Wolff, E.: The EDC3 chronology for the EPICA Dome C ice core, Clim. Past, 3, 485–497, doi:10.5194/cp-3-485-2007, 2007.

Petit, J.-R., Jouzel, J., Raynaud, D., Barkov, N. I., Barnola, J. M., Basile, I., Bender, M., Chappellaz, J., Davis, M., Delaygue, G., Delmotte, M., Kotlyakov, V. M., Legrand, M., Lipenkov, V. Y., Lorius, C., Pepin, L., Ritz, C., Saltzman, E., and Stievenard, M.: Climate and atmospheric history of the past 420 000 years from the Vostok ice core, Antarctica, Nature, 399, 429–436, 1999.

Prokopenko, A. A., Hinnov, L. A., Williams, D. F., and Kuzmin, M. I.: Orbital forcing of continental climate during the Pleistocene: a complete astronomically tuned climatic record from Lake Baikal, SE Siberia, Quaternary Sci. Rev., 25, 3431–3457, Data archived at the World Data Center for Paleoclimatology, Boulder, Colorado, USA, 2006.

Prokopenko, A. A., Karabanov, E. B., Williams, D. F., Kuzmin, M. I., Shackleton, N. J., Crowhurst, S., Peck, J. A., Gvozdkov, A. N., and King, J. W.: Biogenic silica record of the Lake Baikal response to climate forcing during the Brunhes, Quaternary Res., 55, 123–132, 2001.

Raymo, M. E., Oppo, D. W., Flower, B. P., Hodell, D. A., McManus, J. F., Venz, K. A., Kleiven, K. F., and McIntyre, K.: Stability of North Atlantic water masses in face of pronounced climate variability during the Pleistocene, Paleoceanography, 19, Data archived at the World Data Center for Paleoclimatology, Boulder, Colorado, USA, 2004.

Rothlisberger, R., Crosta, X., Abram, N. J., Armand, L., and Wolff, E.: Potential and limitations of marine and ice core sea ice proxies: an example from the Indian Ocean sector, Quaternary Sci. Rev., 29, 296–302, 2010.

Ruddiman, W. F., Raymo, M. E., Martinson, D. G., Clement, B. M., and Backman, J.: Pleistocene evolution: Northern Hemisphere ice sheet and North Atlantic ocean, Paleoceanography, 4(4), 353–412, 1989.

Shackleton, N. J. and Hall, M. A.: Stable isotope history of the Pleistocene at ODP Site 677, Proc. ODP Sci. Res., 111, Data archived at the World Data Center for Paleoclimatology, Boulder, Colorado, USA, 1989.

Sime, L. C., Wolff, E. W., Oliver, K. I. C., and Tindall, J. C.: Evidence for warmer interglacials in East Antarctic ice cores, Nature, 462, 342–345, 2009.

Skinner, L. C. and Shackleton, N. J.: An Atlantic lead over Pacific deep-water change across Termination I: implications for the application of the marine isotope stage stratigraphy, Quaternary Sci. Rev., 24, 571–580, 2005.

Sosdian, S. and Rosenthal, Y.: Deep-Sea Temperature and Ice Volume Changes Across the Pliocene-Pleistocene Climate Transitions, Science, 325, 306–310, Data archived at the World Data Center for Paleoclimatology, Boulder, Colorado, USA, 2009.

Sun, Y. B., and An, Z. S.: History and variability of the Asian interior aridity recorded by eolian flux in the Chinese Loess Plateau during the past 7 Ma, Science in China (Series D), 45(5), 420–429, 2002.

Sun, X., Luo, Y., Huang, F., Tian, J., and Wang, P.: Deep-sea pollen from the South China Sea: Pleistocene indicators of East Asian monsoon, Mar. Geol., 201, 97–118, 2003.

Sun, Y. and An, Z.: Late Pliocene-Pleistocene changes in mass accumulation rates of eolian deposits on the central Chinese Loess Plateau, J. Geophys. Res., 110, Data archived at the World Data Center for Paleoclimatology, Boulder, Colorado, USA, 2005.

Sun, Y., Clemens, S. C., An, Z., and Yu, Z.: Astronomical timescale and palaoeclimatic implications of stacked 3.6-Myr monsoon records from the Chinese Loess Plateau, Quaternary Sci. Rev., 25, 33–48, 2006.

Tian, J., Wang, P., Cheng, X., and Li, Q.: Astronomically tuned Plio-Pleistocene benthic δ^{18}O record from South China Sea and Atlantic-Pacific comparison, Earth Planet. Sc. Lett., 203, 1015–1029, 2002.

Tzedakis, P. C., Hooghiemstra, H., and Palike, H.: The last 1.35 million years at Tenaghi Philippon: revised chronostratigraphy and long-term vegetation trends, Quaternary Sci. Rev., 25, 3416–3430, 2006.

Tzedakis, P. C., Raynaud, D., McManus, J. F., Berger, A., Brovkin, V., and Kiefer, T.: Interglacial diversity, Nat. Geosci., 2, 751–755, 2009.

Venz, K. A. and Hodell, D. A.: A 1.0 Myr record of glacial North Atlantic intermediate water variability from ODP site 982 in the northeast Atlantic, Paleoceanography, 14(1), 42–52, Data archived at the World Data Center for Paleoclimatology, Boulder, Colorado, USA, 1999.

Watanabe, O., Jouzel, J., Johnsen, S., Parrenin, F., Shoji, H., and Yoshida, N.: Homogeneous climate variability across East Antarctica over the past three glacial cycles, Nature, 422, 509–512, 2003.

Wolff, E. W., Barbante, C., Becagli, S., Bigler, M., Boutron, C. F., Castellano, E., De Angelis, M., Federer, U., Fischer, H., Fundel, F., Hansson, M., Hutterli, M., Jonsell, U., Karlin, T., Kaufmann, P., Lambert, F., Littot, G. C., Mulvaney, R., Rothlisberger, R., Ruth, U., Severi, M., Siggaard-Andersen, M. L., Sime, L. C., Steffensen, J. P., Stocker, T. F., Traversi, R., Twarloh, B., Udisti, R., Wagenbach, D., and Wegner, A.: Changes in environment over the last 800 000 years from chemical analysis of the EPICA Dome C ice core, Quaternary Sci. Rev., 29, 285–295, 2010.

Yin, Q. Z. and Berger, A.: Insolation and CO_2 contribution to the interglacial climate before and after the Mid-Brunhes Event, Nat. Geosci., 3, 243–246, 2010.